

Minimax Estimation of Distances on a Surface and Minimax Manifold Learning in the Isometric-to-Convex Setting

Ery Arias-Castro^{*}

Phong Alain Chau[†]

Abstract

We start by considering the problem of estimating intrinsic distances on a smooth submanifold. We show that minimax optimality can be obtained via a reconstruction of the surface, and discuss the use of a particular mesh construction — the tangential Delaunay complex — for that purpose. We then turn to manifold learning and argue that a variant of Isomap where the distances are instead computed on a reconstructed surface is minimax optimal for the isometric variant of the problem.

Keywords: shortest paths, geodesic distances, meshes, tangential Delaunay complex, surfaces with positive reach, manifold learning, Isomap, minimax decision theory

1 Introduction

The estimation of shortest paths and intrinsic distances on surfaces is a fundamental problem in computational geometry with wide-ranging applications. In motion planning, shortest paths represent resource-efficient sequences of actions to be undertaken by the agent in some given configuration space [58, 59]. In addition to the clear applications to robot locomotion and manipulation, this framework has bore fruit in the field of biology wherein proteins and folding networks are of great interest [4, 79]. In cluster analysis, geodesic distances have found use as a similarity metric to create partitions that respect the underlying geometry [53, 60, 67]. In manifold learning (aka nonlinear dimensionality reduction), the Isometric Feature Mapping (Isomap) algorithm crucially depends on the approximation of geodesic distances on the underlying surface [78], and so does another important algorithm, Maximum Variance Unfolding (MVU) [82] — although in disguise [14, 66]. More generally, the estimation of distances is at the core of some important methods for embedding a graph (aka multidimensional scaling) [57, 64, 71, 72].

1.1 Existing error bounds

Consider a set of points $\mathbf{X} = \{x_1, \dots, x_n\}$ in some Euclidean space assumed to belong to some unknown C^2 submanifold \mathcal{M} . The goal is to estimate their pairwise (intrinsic) distances on \mathcal{M} and possibly provide corresponding shortest paths. Therefore, if $d_{\mathcal{M}}$ denotes the intrinsic distance on \mathcal{M} , then the goal is to estimate $d_{\mathcal{M}}(x_i, x_j)$ for all $i, j \in [n] := \{1, \dots, n\}$.

For this goal to be achievable in a nonparametric setting where not much is known about \mathcal{M} except being smooth (see Assumption 3.1 for details) requires that the point set be sufficiently

^{*}Department of Mathematics and Halicioğlu Data Science Institute, University of California, San Diego, USA

[†]Department of Mathematics, University of California, San Diego, USA

dense in \mathcal{M} . To quantify that, suppose¹

$$\max_{x \in \mathcal{M}} \min_{i=1, \dots, n} \|x - x_i\| \leq \varepsilon. \quad (1.1)$$

Note that ε is at best on the order of $(\log(n)/n)^{1/k}$ when the points are sampled uniformly at random from \mathcal{M} and \mathcal{M} is of dimension k . Throughout, we assume that k is known, although this is non-essential as it can be reliably estimated [43, 56].

The first error bounds we know of come from the literature on manifold learning. Indeed, Bernstein *et al* provide some theory for Isomap in [19]. Isomap is based on three main steps: 1) form a neighborhood graph where the nodes are the points and two points within distance r are connected with an edge weighted by the Euclidean distance between the points; 2) compute all the pairwise graph distances; 3) apply Classical Scaling to these distances with a prescribed embedding dimension k . The connectivity radius r is a tuning parameter of the method. Bernstein *et al* focus on the first two steps, meaning on the estimation of the intrinsic distances. Let \mathbf{d}_G denote the graph metric, and note that it depends on r . Bernstein *et al* are able to show that, if \mathcal{M} is geodesically convex and $\varepsilon/r \leq C_1$, then

$$(1 - C_2\varepsilon/r)\mathbf{d}_G(x_i, x_j) \leq \mathbf{d}_{\mathcal{M}}(x_i, x_j) \leq (1 + C_2r^2)\mathbf{d}_G(x_i, x_j), \quad \forall i, j \in [n], \quad (1.2)$$

where C_1, C_2 are constants depending on \mathcal{M} .

The assumption of geodesic convexity is in fact not needed for (1.2) to hold as long as the shortest paths on \mathcal{M} have curvature bounded by some C depending on \mathcal{M} , as shown in [12]. In that paper, the upper bound is derived based on the seminal work of Dubins [39] (the lower bound can be obtained by elementary means), and the problem is also considered under a curvature constraint on the paths. The lower bound (1.2) is derived independently by Oh *et al* [65] in the context of a convex domain, motivated by the problem of placing sensors that are only aware of other sensors within a prescribed distance — one variant of the sensor network localization problem. Note that the upper bound $\mathbf{d}_{\mathcal{M}}(x_i, x_j) \leq \mathbf{d}_G(x_i, x_j)$ holds in that case. In the same setting, Janson *et al* [51] derive a similar lower bound in the context of path planning in robotics in the presence of obstacles (although with some clearance) and where again the upper bound is trivial. Arias-Castro *et al* [11] sharpen the lower bound, replacing ε/r with $(\varepsilon/r)^2$. They do so in the more general setting where \mathcal{M} is isometric to a convex domain.

In summary, for general C^2 submanifolds, the best available bound remains (1.2) as established recently in [12]. And if one optimizes the bounds in terms of r (the tuning parameter here) — a task that in principle requires knowledge of ε — we find that the relative error rate is in $O(\varepsilon^{2/3})$, specifically,

$$|\mathbf{d}_{\mathcal{M}}(x_i, x_j) - \mathbf{d}_G(x_i, x_j)| \leq C\varepsilon^{2/3}\mathbf{d}_{\mathcal{M}}(x_i, x_j), \quad \forall i, j \in \{1, \dots, n\}, \quad (1.3)$$

where C is a constant that depends on \mathcal{M} . In fact, this rate already appears in [3]. If \mathcal{M} is isometric to a convex domain, the improved result in [11] leads to a relative error rate in $O(\varepsilon)$.

Remark 1.1. Note that in sensor network localization [65] and in path planning [51], the quantity r is typically *not* a parameter that the user can change. We are here in the original context of points in space, as in manifold learning.

¹The use of intrinsic distances could be used instead, but this would not change things in any noticeable way.

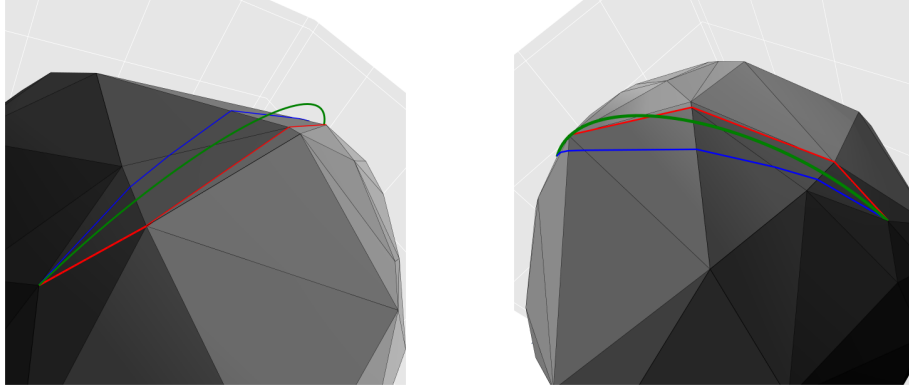


Figure 1.1: A setting where the underlying surface is a sphere. The shortest path on the surface (green), on the mesh (blue), and on the neighborhood graph (red), between two sample points are shown.

1.2 A new error bound

It turns out that (1.3) is far from optimal. Indeed, we show that it is possible to obtain estimates \hat{d}_{ij} such that

$$|\mathbf{d}_{\mathcal{M}}(x_i, x_j) - \hat{d}_{ij}| \leq C\varepsilon^2 \min\{\mathbf{d}_{\mathcal{M}}(x_i, x_j), \hat{d}_{ij}\}, \quad \forall i, j \in [n], \quad (1.4)$$

where C is again a generic constant depending on \mathcal{M} .

We first propose a non-constructive approach that consists in interpolating the data points by a smooth surface, and then estimating the distance on \mathcal{M} by the distance on that interpolating surface.

We then propose a more practical approach based instead on a mesh construction. The particular mesh construction that we use is the tangential Delaunay complex [21, 24, 25, 42]. In fact, because it requires knowledge of the tangent subspaces to the surface \mathcal{M} at the sample points, we follow Aamari and Levrard [2] and first estimate the tangent spaces. See Figure 1.1 for an illustration.

In addition to proposing estimators that satisfy the performance bound (1.4), we show that the relative error rate in $O(\varepsilon^2)$ that results from that bound is best possible in an information-theoretic sense — even if we know that \mathcal{M} is isometric to a convex domain.

Remark 1.2. Experts in computational geometry are aware of approximating meshes providing an approximation to the metric on the surface. For example, the paper [40] provides sufficient conditions for a mesh construction to satisfy an approximation bound like our Theorem 3.3.² This result is used in [22] to derive a bound similar to (1.4) for a mesh construction based on knowledge of an atlas of the underlying surface \mathcal{M} . Here we show that knowledge of underlying surface is in fact not needed — an important difference as we adopt an estimation/information-theoretic stance.

²[40, Th 3], as stated, provides a distortion bound in $O(1)$, which is of course less than satisfactory. However, a quick inspection reveals that, with the notation of that paper, one can take $h \leq h_0 := \min\{\iota_{\mathcal{M}}/4, t_0/6\sqrt{\Lambda}\}$ instead of $h = h_0$ as stated in the result, leading to a bound in $O(h^2)$, which is of similar order as (1.4) as h there plays the role of ε here. We note in passing that the sufficient conditions provided in that theorem for a mesh to provide a good metric approximation rely on knowing the underlying surface.

Remark 1.3. After our work was made public, Aamari, Berenfeld and Levrard [1] obtained minimax bounds on the estimation of the metric of a C^q submanifold based on a sample drawn iid from a density supported on the submanifold. Although the setting is a little different, the bound is also in $O(\varepsilon^2)$ when $q = 2$.

1.3 Application: minimax manifold learning

We already mentioned one of the main methods for manifold learning, Isomap [78], which consists in estimating the pairwise intrinsic distances by shortest path distances in a neighborhood graph, followed by an application of Classical Scaling. Arias-Castro *et al* [11] derive an error bound for Isomap based on a perturbation bound for Classical Scaling.

An improved estimation of the pairwise intrinsic distances naturally leads to an improved performance. We show that the resulting performance bound — obtained by a combination of the new bound (1.4) and perturbation bounds available in [11] — is optimal in an information-theoretic sense for the problem of manifold learning in the setting where the submanifold \mathcal{M} is isometric to a convex domain.

In its more practical form, where a mesh reconstruction of the surface is used, we call the resulting method *Mesh Isomap*. This idea of using a mesh to improve on Isomap is not entirely new and is brought up in a discussion [15] of the main Isomap paper [78]. We elaborate on this point in Remark 5.9.

1.4 Content

The rest of the paper is organized as follows. In Section 2, we list or quickly derive some results that will prove useful later on in the paper. In Section 3, we derive an estimator that satisfies the announced performance bound (1.4). We also show that this cannot be improved upon from an information-theoretic perspective. While the estimator defined and studied in that section is not constructive, in Section 4 we propose a more practical alternative based on a particular mesh construction — the tangential Delaunay complex — which we show achieves the same level of performance. We show the method in action in some numerical experiments. In Section 5, we turn to the problem of (isometric) manifold learning and apply the conclusions of the previous sections to derive a minimax optimal procedure and showcase Mesh Isomap in some numerical experiments. Section 6 is a brief discussion section.

2 Preliminaries

In this section we introduce some concepts and tools that will be used in subsequent sections to derive the main results.

2.1 Length of a curve

Before proceeding, we recall that a curve in \mathbb{R}^d can be defined as the range of a continuous function $\gamma : [0, 1] \rightarrow \mathbb{R}^d$. We may identify a curve γ with one of its parameterization without warning. The length of a curve γ is defined as

$$\Lambda(\gamma) := \sup \sum_j \|\gamma(t_{j+1}) - \gamma(t_j)\|,$$

where the supremum is over all increasing sequences $(t_j) \subset [0, 1]$. We also note that, if \mathcal{M} is a closed topological submanifold of a Euclidean space without boundary,³ then for each pair of points $x, x' \in \mathcal{M}$ there is a shortest path on \mathcal{M} joining them, meaning that the following infimum is attained

$$\inf \{ \Lambda(\gamma) \mid \gamma : [0, 1] \rightarrow \mathcal{M}, \gamma(0) = x, \gamma(1) = x' \}.$$

The following is by definition of parameterization by arc length.

Lemma 2.1. *Consider a differentiable and injective function $\gamma : [0, 1] \rightarrow \mathbb{R}^d$. For $t \in [0, 1]$, let $\lambda(t)$ denote the length of $\gamma([0, t]) = \{\gamma(s) : 0 \leq s \leq t\}$. Then there is a differentiable and injective function $\nu : [0, \Lambda(\gamma)] \rightarrow \mathbb{R}^d$ differentiable such that $\nu(\lambda(t)) = \gamma(t)$ for all $t \in [0, 1]$. Since satisfies $\|\dot{\nu}(s)\| = 1$ for all s , ν is an isometric diffeomorphism between $[0, \Lambda(\gamma)]$ and $\gamma([0, 1])$.*

2.2 Distortion maps

A map $F : U \rightarrow \mathbb{R}^d$, where $U \subset \mathbb{R}^p$ where p and d may be different, is called a ξ -distortion map if

$$\|F(x) - F(y)\| - \|x - y\| \leq \xi \|x - y\|, \quad \forall x, y \in U.$$

Note that a ξ -distortion map is Lipschitz with constant $(1 + \xi)$, and if $\xi < 1$, it is injective and its inverse (defined on its range) is also Lipschitz with constant $(1 - \xi)^{-1}$, and in fact, a $\xi/(1 - \xi)$ -distortion map. This is important because of the following.

Lemma 2.2. *For any curve γ and any L -Lipschitz function F , $\Lambda(F(\gamma)) \leq L \Lambda(\gamma)$. As a consequence, if F is a ξ -distortion map with $\xi < 1$, then for any curve γ ,*

$$|\Lambda(\gamma) - \Lambda(F(\gamma))| \leq \frac{\xi}{1 - \xi} \min\{\Lambda(\gamma), \Lambda(F(\gamma))\}. \quad (2.1)$$

Proof. We provide a proof for completeness. For the first part, we first note that $F(\gamma) = F \circ \gamma$ is indeed a curve. Also, for an increasing sequence $(t_j) \subset [0, 1]$, we have

$$\sum_j \|F \circ \gamma(t_{j+1}) - F \circ \gamma(t_j)\| \leq \sum_j L \|\gamma(t_{j+1}) - \gamma(t_j)\|,$$

and taking the supremum over all such sequences leads to the desired bound.

For the second part, meaning (2.1), from the first part we obtain $\Lambda(F(\gamma)) \leq (1 + \xi)\Lambda(\gamma)$ since F is $(1 + \xi)$ -Lipschitz. Let $\eta = F(\gamma)$. Then F^{-1} is obviously defined on η , and being $(1 - \xi)^{-1}$ -Lipschitz, the first part gives $\Lambda(F^{-1}(\eta)) \leq (1 - \xi)^{-1}\Lambda(\eta)$, or equivalently, $\Lambda(\gamma) \leq (1 - \xi)^{-1}\Lambda(F(\gamma))$. This gives the first inequality in (2.1). Two cases are possible. If $\Lambda(\gamma) \geq \Lambda(F(\gamma))$, then we use the first inequality to get

$$0 \leq \Lambda(\gamma) - \Lambda(F(\gamma)) \leq (1 + \xi)\Lambda(\gamma) - \Lambda(\gamma) = \xi\Lambda(\gamma).$$

If $\Lambda(\gamma) \leq \Lambda(F(\gamma))$, then we use the second inequality to get

$$0 \leq \Lambda(F(\gamma)) - \Lambda(\gamma) \leq (1 - \xi)^{-1}\Lambda(\gamma) - \Lambda(\gamma) = \frac{\xi}{1 - \xi}\Lambda(\gamma).$$

In either case, (2.1) is implied. □

³This properties is also satisfied by topological submanifolds with boundary under some conditions on the boundary. We focus on submanifolds without boundary as these are the objects that occupy us in the present paper.

The following is a simple corollary of this lemma. Although straightforward, it is at the very root of this idea of using a surface reconstruction to obtain better approximating rates for the intrinsic distances. In what follows, \mathcal{S} should be thought of as playing the role of approximating surface to \mathcal{M} , even as they in fact play symmetric roles.

Corollary 2.3. *Suppose that $\mathcal{S} \subset \mathbb{R}^p$ is a closed topological submanifold without boundary and that $F : \mathcal{S} \rightarrow \mathbb{R}^d$ is some ξ -distortion map with $\xi < 1$. Then $\mathcal{M} := F(\mathcal{S}) \subset \mathbb{R}^d$ is also a closed topological submanifold without boundary. Moreover, the distance on \mathcal{M} can be approximated by the distance on \mathcal{S} to within a relative error of $(1 - \xi)^{-1}$ in the sense that*

$$|\mathrm{d}_{\mathcal{M}}(x, x') - \mathrm{d}_{\mathcal{S}}(F^{-1}(x), F^{-1}(x'))| \leq \frac{\xi}{1 - \xi} \min\{\mathrm{d}_{\mathcal{M}}(x, x'), \mathrm{d}_{\mathcal{S}}(F^{-1}(x), F^{-1}(x'))\}, \quad \forall x, x' \in \mathcal{M}.$$

Proof. The fact that \mathcal{M} is a closed topological submanifold without boundary is because \mathcal{S} satisfies these properties by assumption and F is a homeomorphism between \mathcal{S} and \mathcal{M} . Now, take $x, x' \in \mathcal{M}$, and let γ be a shortest path on \mathcal{S} between $y := F^{-1}(x)$ and $y' := F^{-1}(x')$ so that $\mathrm{d}_{\mathcal{S}}(y, y') = \Lambda(\gamma)$. Applying Lemma 2.2, using the fact that F is $(1 + \xi)$ -Lipschitz, we have that $\Lambda(F(\gamma)) \leq (1 + \xi)\Lambda(\gamma)$. And since $F(\gamma) = F \circ \gamma$ is a curve on \mathcal{M} between x and x' , we have $\mathrm{d}_{\mathcal{M}}(x, x') \leq \Lambda(F(\gamma))$. We thus have

$$\mathrm{d}_{\mathcal{M}}(x, x') \leq \Lambda(F(\gamma)) \leq (1 + \xi)\Lambda(\gamma) = (1 + \xi)\mathrm{d}_{\mathcal{S}}(y, y').$$

Similarly, using the fact that F^{-1} is $(1 - \xi)^{-1}$ -Lipschitz, we obtain

$$\mathrm{d}_{\mathcal{S}}(y, y') \leq (1 - \xi)^{-1}\mathrm{d}_{\mathcal{M}}(x, x').$$

We conclude combining these two bounds. □

2.3 Medial axis, reach, and metric projection

The medial axis of \mathcal{M} , denoted $\mathrm{ax}(\mathcal{M})$, is the set of points in \mathbb{R}^d that have two or more closest points on \mathcal{M} . We define the (metric) projection onto \mathcal{M} as $P_{\mathcal{M}} : \mathbb{R}^d \setminus \mathrm{ax}(\mathcal{M}) \rightarrow \mathcal{M}$ that sends a point x to its (unique) closest point on \mathcal{M} . The reach of \mathcal{M} the infimum of the distance between a point in \mathcal{M} and $\mathrm{ax}(\mathcal{M})$ [41]. It is well-known that a compact connected C^2 submanifold without boundary has a (strictly) positive reach, and that the inverse of the reach bounds from above the (sectional) curvature on \mathcal{M} , pointwise.

Recall that the h -tubular neighborhood of $\mathcal{M} \subset \mathbb{R}^d$ is the set of all points that are within distance h of \mathcal{M} , meaning $\{x : \mathrm{dist}(x, \mathcal{M}) \leq h\}$.

Lemma 2.4 (Th 4.8(8) in [41]; Lem 7.13 in [21]). *If \mathcal{M} has reach $\geq \rho$, then for any $h < \rho$, $P_{\mathcal{M}}$ is $\rho/(\rho - h)$ -Lipschitz on the h -tubular neighborhood of \mathcal{M} .*

Lemma 2.5. *If \mathcal{M} and \mathcal{S} have reach $\geq \rho$ and are within Hausdorff distance $h \leq \rho/2$, then*

$$|\mathrm{d}_{\mathcal{M}}(x, x') - \mathrm{d}_{\mathcal{S}}(x, x')| \leq (2h/\rho) \min\{\mathrm{d}_{\mathcal{M}}(x, x'), \mathrm{d}_{\mathcal{S}}(x, x')\}, \quad \forall x, x' \in \mathcal{M} \cap \mathcal{S}.$$

Proof. Let γ be a shortest path on \mathcal{M} between x and x' , so that $\Lambda(\gamma) = \mathrm{d}_{\mathcal{M}}(x, x')$. Because $\gamma \subset \mathcal{M}$, γ is entirely in the h -tubular neighborhood of \mathcal{S} , and we may define $\zeta := P_{\mathcal{S}}(\gamma)$, which is a curve on \mathcal{S} joining x and x' . In particular, $\mathrm{d}_{\mathcal{S}}(x, x') \leq \Lambda(\zeta)$. The fact that γ is entirely in the h -tubular neighborhood of \mathcal{S} also implies via Lemma 2.4 that $P_{\mathcal{S}}$ is $(1 + \xi)$ -Lipschitz on γ with $\xi := h/(\rho - h)$, in turn implying via Lemma 2.2 that $\Lambda(\zeta) \leq (1 + \xi)\Lambda(\gamma)$. We have thus established that $\mathrm{d}_{\mathcal{S}}(x, x') \leq (1 + \xi)\mathrm{d}_{\mathcal{M}}(x, x')$.

The reverse inequality holds by symmetry, given that \mathcal{M} and \mathcal{S} play the same role, and applying these two bounds together with the fact that $h \leq \rho/2$ — which implies that $\xi \leq 2h/\rho$ — yields

$$d_{\mathcal{S}}(x, x') - d_{\mathcal{M}}(x, x') \leq \frac{2h}{\rho} d_{\mathcal{M}}(x, x') \quad \text{and} \quad d_{\mathcal{M}}(x, x') - d_{\mathcal{S}}(x, x') \leq \frac{2h}{\rho} d_{\mathcal{S}}(x, x'),$$

from which the result follows immediately. \square

2.4 Simplexes

A finite subset σ of a Euclidean space is said to be a k -simplex if σ is the convex hull of $k+1$ affinely independent points. The thickness $\tau(\sigma)$ of a k -simplex σ is defined as the ratio of its smallest altitude to its diameter. (A slightly different definition is given in [21], but the two notions are proportional to each other.)

The thickness of a simplex is a measure of its regularity in that a lower bound on the thickness implies a lower bound on the angles of the simplex, and also on the ratio of the lengths of its shortest and longest edges. In particular, a regular k -simplex has the largest possible thickness among all k -simplexes, equal to $\tau_k := \sqrt{(k+1)/2k}$.

The thickness of a simplex σ can also be measured based on its side length ratio $\pi(\sigma)$, defined as the length of its shortest edge divided by the length of its longest edge. Indeed, the following (straightforward) result holds.

Lemma 2.6. *There is an increasing homeomorphism ϕ_k of $[0, 1]$ such that $\tau(\sigma) \geq \tau_k \phi_k(\pi(\sigma))$ for any k -simplex σ .*

2.5 Affine subspaces

Affine subspaces will play an important role in the form of tangent spaces. We will need the following bounds on the angle between affine subspaces. For two such subspaces, T and T' , we denote by $\angle(T, T')$ their angle, or more precisely, their maximum principal (aka canonical) angle [76, Sec I.5.2].

The first result is referred to as Whitney's angle bound in [21].

Lemma 2.7 (Lem 15c in [84] or Lem 5.14 in [21]). *Let T be an affine subspace and let σ be a k -simplex whose edges are all of length at least η and whose vertices are all within distance δ of T . Then*

$$\sin \angle(\text{aff}(\sigma), T) \leq \frac{2}{(k-1)!} \frac{\delta}{\tau(\sigma)\eta},$$

where $\text{aff}(\sigma)$ is the affine subspace generated by the vertices of σ .

In the next result, we compare the distances of a point to two intersecting affine subspaces based on the angle between these subspaces.

Lemma 2.8. *For two intersecting affine subspaces T and T' , and any point x ,*

$$|\text{dist}(x, T) - \text{dist}(x, T')| \leq \angle(T, T') \text{dist}(x, T \cap T').$$

Proof. Let $t \in T$, $t' \in T'$, and $y \in T \cap T'$ be closest to x in their respective set. Define the angles

$$\theta = \angle((xy), (ty)) = \angle((xy), T), \quad \theta' = \angle((xy), (t'y)) = \angle((xy), T').$$

Then $\text{dist}(x, T) = \sin(\theta)\|x - y\|$ and $\text{dist}(x, T') = \sin(\theta')\|x - y\|$, so that

$$|\text{dist}(x, T) - \text{dist}(x, T')| \leq |\sin \theta - \sin \theta'| \|x - y\|.$$

We conclude with

$$|\sin \theta - \sin \theta'| \leq |\theta - \theta'| \leq \angle(T, T'),$$

by the triangle inequality for angles between subspaces, combined with

$$\|x - y\| \leq \text{dist}(x, T \cap T'),$$

due to the simple fact that $y \in T \cap T'$. □

Let P_T denote the orthogonal projection onto the affine subspace T (which is also the metric projection onto T). Also, for matrix A , let $\|A\|$ denote the operator norm of A . The following is well-known [76, Sec I.5.2].

Lemma 2.9. *For two linear subspaces T and T' of same dimension, $\|P_T - P_{T'}\| = \sin \angle(T, T')$. Moreover, $\min\{\|U - I\| : U \text{ orthogonal, } UT = T'\} = 2 \sin(\frac{1}{2} \angle(T, T'))$.*

2.6 Tangent spaces

For a submanifold \mathcal{M} , we let $T_{\mathcal{M}}(x)$ denote the tangent space of \mathcal{M} at $x \in \mathcal{M}$. A lot is known about the tangent spaces of a submanifold with positive reach and their orthogonal projections.

The first result is on the distance of a point on the surface to a tangent space at some other point on the surface, and conversely, on the distance of a point on a tangent space to the surface.

Lemma 2.10 (Th 4.18 in [41]; Lem 7.8(2) in [21]; Lem 2 in [13]). *Let \mathcal{M} be a submanifold with reach at least $r > 0$. For $x, x' \in \mathcal{M}$, $\text{dist}(x', T_{\mathcal{M}}(x)) \leq \frac{1}{2r}\|x - x'\|^2$. Moreover, if $t \in T_{\mathcal{M}}(x)$ is such that $\|t - x\| \leq r/3$, then $\text{dist}(t, \mathcal{M}) \leq \frac{1}{r}\|t - x\|^2$.*

The second result is on the distortion of the projection onto a tangent space restricted to a neighborhood of the surface around the point of contact.

Lemma 2.11 (Lem 7.14(1) in [21] and Lem 5 in [13]). *Let \mathcal{M} be a submanifold with reach at least $r > 0$. For any $h < r/2$ and any $x \in \mathcal{M}$, the restriction to $B(x, h) \cap \mathcal{M}$ of the orthogonal projection onto the tangent space at x is a $4(h/r)^2$ -distortion map. Moreover the projection of $B(x, h) \cap \mathcal{M}$ contains $B(x, h - Ch^3) \cap T_{\mathcal{M}}(x)$ for a constant C that depends only on \mathcal{M} .*

3 Minimax metric estimation

The basic idea leading to our new bound (1.4) is to reconstruct the surface, at least approximately, and then compute the shortest paths between the sample points on the reconstructed surface. In our case, it turns out that the reconstructed surface interpolates the sample points, but this is not necessary in principle.

3.1 Metric estimation by surface reconstruction

In this subsection, we are in a setting where we have a set of points $\mathbf{X} = \{x_1, \dots, x_n\} \subset \mathbb{R}^d$ assumed, as in (1.1), to be an ε -covering of a set $\mathcal{M} \subset \mathbb{R}^d$ satisfying the following properties:

Assumption 3.1. \mathcal{M} is a compact and connected k -dimensional C^2 submanifold without boundary.

See Remark 3.6 for extensions.

Our main goal is to define a surface $\hat{\mathcal{M}}$ interpolating the same points and with similar characteristics. This surface will approximate \mathcal{M} well enough that the distances on $\hat{\mathcal{M}}$ will be good approximations to the distances on \mathcal{M} . The approach for defining $\hat{\mathcal{M}}$ is not constructive, but rather relies on the axiom of choice. We present an actual construction in Section 4 based on recent developments in computational geometry. Our definition here is much more elementary and is enough to establish the achievability of (1.4), at least from an information-theoretic perspective.

Let $\mathbb{M} = \mathbb{M}(k, \mathbf{X}, \varepsilon)$ denote the class of submanifolds satisfying Assumption 3.1 for which \mathbf{X} is an ε -covering. We know that \mathbb{M} is non-empty since $\mathcal{M} \in \mathbb{M}$. Let ρ_{\max} denote the supremum reach among surfaces in \mathbb{M} . Select any surface⁴ $\hat{\mathcal{M}}$ in \mathbb{M} with reach $\rho(\hat{\mathcal{M}}) \geq \rho_{\max}/2$, so that $\rho(\hat{\mathcal{M}}) \geq \rho(\mathcal{M})/2$. The surface $\hat{\mathcal{M}}$ offers a good approximation to \mathcal{M} , as the following result establishes.

Proposition 3.2. *There is C which only depends on \mathcal{M} such that $\text{dist}(\mathcal{M}, \hat{\mathcal{M}}) \leq C\varepsilon^2$.*

With the interpolating surface $\hat{\mathcal{M}}$ defined, we estimate the metric on \mathcal{M} by the metric on $\hat{\mathcal{M}}$. Therefore, define the estimator

$$\hat{d}_{ij} := d_{\hat{\mathcal{M}}}(x_i, x_j), \quad \forall i, j \in [n]. \quad (3.1)$$

Theorem 3.3. *There is a constant C that only depends on \mathcal{M} such that, whenever $\varepsilon \leq 1/C$,*

$$|d_{\mathcal{M}}(x, x') - d_{\hat{\mathcal{M}}}(x, x')| \leq C\varepsilon^2 \min\{d_{\mathcal{M}}(x, x'), d_{\hat{\mathcal{M}}}(x, x')\}, \quad \forall x, x' \in \mathcal{M} \cap \hat{\mathcal{M}}.$$

This implies that the estimator defined in (3.1) satisfies (1.4).

Proof. Let C_0 be the constant of Proposition 3.2. Suppose that ε is small enough that $C_0\varepsilon^2 \leq \rho(\mathcal{M})/4$. Because $\rho(\hat{\mathcal{M}}) \geq \rho(\mathcal{M})/2$ by construction, we have $\text{dist}(\mathcal{M}, \hat{\mathcal{M}}) \leq \frac{1}{2} \min\{\rho(\mathcal{M}), \rho(\hat{\mathcal{M}})\}$, which allows us to apply Lemma 2.5 and conclude. \square

We now turn to the proof of Proposition 3.2. In what follows, C, C_1, C_2, \dots are generic constants that only depend on \mathcal{M} and may change with each appearance.

Lemma 3.4. *In the present situation, whenever $\varepsilon \leq 1/C$, for every $x \in \mathcal{M}$, there are sample points x_{i_1}, \dots, x_{i_k} such that the k -simplex defined by $\{x, x_{i_1}, \dots, x_{i_k}\}$ has minimum side length $\geq \varepsilon$ and thickness $\geq 1/C$.*

Proof. Let T be shorthand for $T_{\mathcal{M}}(x)$. For $A > 0$ to be chosen large enough later, pick $t_1, \dots, t_k \in T$ such that the convex hull of $\{x, t_1, \dots, t_k\}$ is a regular k -simplex of side length $A\varepsilon$. By Lemma 2.11, the resulting map is one-to-one on $B(x, h) \cap \mathcal{M}$ whenever $h < \rho(\mathcal{M})/2$. We restrict P_T to that set, and for each q , define $u_q = P_T^{-1}(t_q)$ so that $u_q \in B(x, h) \cap \mathcal{M}$. In particular, since $u_q \in \mathcal{M}$, we have $\|t_q - u_q\| \leq \text{dist}(t_q, \mathcal{M})$. Noting that $\|t_q - x\| = A\varepsilon$, by Lemma 2.10 there is $C_1 > 0$ such that, if $A\varepsilon \leq 1/C_1$, then $\text{dist}(t_q, \mathcal{M}) \leq C_1(A\varepsilon)^2$.

⁴If there is a surface in \mathbb{M} with reach ρ_{\max} , it is natural to choose such a surface. We believe this is possible, but we are not sure. In any case, what matters is that the regularity of $\hat{\mathcal{M}}$ is controlled as a function of \mathcal{M} .

For each q , let x_{i_q} be a sample point satisfying $\|u_q - x_{i_q}\| \leq \varepsilon$, which exists by virtue of the fact that $u_q \in \mathcal{M}$ by construction and the sample points form an ε -covering of \mathcal{M} by assumption. Let σ denote the simplex defined by $\{x, x_{i_1}, \dots, x_{i_k}\}$, meaning the convex hull of that point set. Then, by the triangle inequality, σ has side lengths satisfying

$$\begin{aligned} \|x_{i_q} - x_{i_p}\| &\leq \|x_{i_q} - u_q\| + \|u_q - t_q\| + \|t_q - t_p\| + \|t_p - u_p\| + \|u_p - x_{i_p}\| \\ &\leq \varepsilon + C_1(A\varepsilon)^2 + A\varepsilon + C_1(A\varepsilon)^2 + \varepsilon \\ &= A\varepsilon(1 + 2/A + 2C_1A\varepsilon), \end{aligned}$$

and

$$\begin{aligned} \|x_{i_q} - x_{i_p}\| &\geq -\|x_{i_q} - u_q\| - \|u_q - t_q\| + \|t_q - t_p\| - \|t_p - u_p\| - \|u_p - x_{i_p}\| \\ &\geq -\varepsilon - C_1(A\varepsilon)^2 + A\varepsilon - C_1(A\varepsilon)^2 - \varepsilon \\ &= A\varepsilon(1 - 2/A - 2C_1A\varepsilon), \end{aligned}$$

and the same upper and lower bounds apply when x replaces x_{i_q} above. Therefore, σ has minimum side length $\geq A\varepsilon(1 - 2/A - 2C_1A\varepsilon)$ and side length ratio

$$\pi(\sigma) \geq \frac{1 - 2/A - 2C_1A\varepsilon}{1 + 2/A + 2C_1A\varepsilon}.$$

We first require that $A \geq 4$ and $A\varepsilon \leq 1/8C_1$, so that σ has minimum side length $\geq \varepsilon$. Recall the definition of ϕ_k in Lemma 2.6. Since $\tau_k > 1/\sqrt{2}$, there is C_2 such that $\phi_k(1 - 1/C_2) = 1/(\sqrt{2}\tau_k)$. Choose $A \geq 4$ large enough that $(1 - 2A)/(1 + 2A) \geq 1 - 1/2C_2$, and then ε small enough that $A\varepsilon \leq 1/8C_1$ (as required above) and $(1 - 2/A - 2C_1A\varepsilon)/(1 + 2/A + 2C_1A\varepsilon) \geq 1 - C_2$. In that case, the simplex σ constructed above is such that $\pi(\sigma) \geq 1 - 1/C_2$, which via Lemma 2.6 implies that $\tau(\sigma) \geq \tau_k\phi_k(1 - 1/C_2) = 1/\sqrt{2}$. \square

Lemma 3.5. *In the present situation, for every $x \in \mathcal{M} \cap \hat{\mathcal{M}}$, $\angle(T_{\mathcal{M}}(x), T_{\hat{\mathcal{M}}}(x)) \leq C\varepsilon$.*

Proof. Take any point $x \in \mathcal{M} \cap \hat{\mathcal{M}}$ and consider the point set x_{i_1}, \dots, x_{i_k} defined in Lemma 3.4. By Lemma 2.10,

$$\text{dist}(x_{i_q}, T_{\mathcal{M}}(x)) \leq C_1\|x_{i_q} - x\|^2 \leq C_2\varepsilon^2.$$

Using Lemma 2.7, we have that

$$\sin \angle(\text{aff}(\sigma), T_{\mathcal{M}}(x)) \leq A \frac{C_2\varepsilon^2}{(1/C_0)\varepsilon} =: C_3\varepsilon,$$

where A is a universal constant and C_0 is the constant of Lemma 3.4. Similarly,

$$\sin \angle(\text{aff}(\sigma), T_{\hat{\mathcal{M}}}(x)) \leq C_4\varepsilon.$$

(In principle C_4 would depend on $\hat{\mathcal{M}}$, but a more careful tracking of the constants reveal that they really only depend on a lower bound on the reach of the underlying surface, and $\rho(\hat{\mathcal{M}}) \geq \rho(\mathcal{M})/2$ by construction.) We then conclude by the triangle inequality that

$$\begin{aligned} \angle(T_{\mathcal{M}}(x), T_{\hat{\mathcal{M}}}(x)) &\leq \angle(T_{\mathcal{M}}(x), \text{aff}(\sigma)) + \angle(\text{aff}(\sigma), T_{\hat{\mathcal{M}}}(x)) \\ &\leq \frac{\pi}{2}C_3\varepsilon + \frac{\pi}{2}C_4\varepsilon =: C_5\varepsilon, \end{aligned}$$

using the fact that $\sin a \geq \frac{2}{\pi}a$ for all $a \in [0, \frac{\pi}{2}]$. \square

Proof of Proposition 3.2. Take $x \in \mathcal{M}$. We want to show that $\text{dist}(x, \hat{\mathcal{M}}) \leq C\varepsilon^2$. Let x_i be such that $\|x - x_i\| \leq \varepsilon$. Then by Lemma 2.10, we have $\text{dist}(x, T_{\mathcal{M}}(x_i)) \leq C_1\varepsilon^2$. Also, by Lemma 2.8,

$$\begin{aligned} \text{dist}(x, T_{\hat{\mathcal{M}}}(x_i)) &\leq \text{dist}(x, T_{\mathcal{M}}(x_i)) + \angle(T_{\mathcal{M}}(x_i), T_{\hat{\mathcal{M}}}(x_i)) \text{dist}(x, T_{\mathcal{M}}(x_i) \cap T_{\hat{\mathcal{M}}}(x_i)) \\ &\leq C_1\varepsilon^2 + (C_2\varepsilon)\|x - x_i\| \leq C_3\varepsilon^2, \end{aligned}$$

using Lemma 3.5 with C_2 denoting the constant there. Let t be the orthogonal projection of x onto $T_{\hat{\mathcal{M}}}(x_i)$ so that $\|x - t\| \leq C_3\varepsilon^2$. We have

$$\begin{aligned} \|x_i - t\| &\leq \|x_i - x\| + \|x - t\| \\ &\leq \varepsilon + \text{dist}(x, T_{\hat{\mathcal{M}}}(x_i)) \\ &\leq \varepsilon + C_3\varepsilon^2 \leq C_4\varepsilon. \end{aligned}$$

By Lemma 2.10, if $C_4\varepsilon \leq 1/C_5$, then $\text{dist}(t, \hat{\mathcal{M}}) \leq C_5(C_4\varepsilon)^2 =: C_6\varepsilon^2$. (C_5 depends monotonically on $\rho(\hat{\mathcal{M}})$, but $\rho(\hat{\mathcal{M}}) \geq \rho(\mathcal{M})/2$ by construction.) Finally, by the triangle inequality,

$$\text{dist}(x, \hat{\mathcal{M}}) \leq \|x - t\| + \text{dist}(t, \hat{\mathcal{M}}) \leq C_3\varepsilon^2 + C_6\varepsilon^2 =: C_7\varepsilon^2.$$

Similarly, we can show that for any $s \in \hat{\mathcal{M}}$, $\text{dist}(s, \mathcal{M}) \leq C_8\varepsilon^2$, and combined, this allows us to conclude that $\text{dist}(\mathcal{M}, \hat{\mathcal{M}}) \leq \max\{C_7, C_8\}\varepsilon^2$. \square

Remark 3.6. Although we have followed the tradition of working with submanifolds without boundary, an extension to submanifolds with boundary is straightforward albeit a little more tedious. Indeed, all the steps in the proof of Theorem 3.3 apply to surfaces with boundary, except possibly for Lemma 3.4. For this lemma to apply, it is enough that $\partial\mathcal{M}$ is itself smooth or that it does not have arbitrarily ‘sharp’ singularities. Technically, it is enough that, for some constant $\alpha = \alpha(\mathcal{M}) > 0$, for each $x \in \mathcal{M}$ and $h \leq \alpha$, the orthogonal projection of $B(x, h) \cap \mathcal{M}$ onto $T_{\mathcal{M}}(x)$ contains a cone of the form

$$\{t \in T_{\mathcal{M}}(x) \cap B(x, \alpha h) : \angle(t - x, u) \leq \alpha\},$$

for some normed vector u . This condition applies, for example, to the situation where $\partial\mathcal{M}$ is itself a C^2 submanifold, or more generally, when it is locally the graph of a Lipschitz function.

3.2 Information bound

So far, we have worked in a setting where all we know about the underlying surface \mathcal{M} satisfies Assumption 3.1. Based on this, we have defined an estimator that satisfies the error bound (1.4). The question arises: Is this best possible? We approach this question from a minimax perspective, and it turns out it is indeed best possible.

Our approach is standard: the idea is to construct a situation where two distinct surfaces satisfying Assumption 3.1 with sufficiently different metrics and that interpolate the same set of points. For other examples in the geometrical statistics literature, see [1, 2, 37, 44, 55]. We work with surfaces that have a boundary, knowing that we can extend them into surfaces without boundary without modifying the construction in any otherwise meaningful way.

In the next subsections, we prove the following information lower bound. (In fact, we prove a somewhat stronger result.)

Theorem 3.7. *For any estimator \hat{d} , the following is true. For any $\varepsilon > 0$, there is a surface \mathcal{M} satisfying Assumption 3.1 and a set of points x_1, \dots, x_n belonging to \mathcal{M} dense enough that (1.1) holds, such that the proportion of pairs $i \neq j$ for which*

$$|\hat{d}_{ij} - d_{\mathcal{M}}(x_i, x_j)| \geq C^{-1}\varepsilon^2 d_{\mathcal{M}}(x_i, x_j)$$

approaches 1 as C increases without bound.

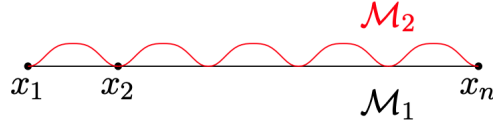


Figure 3.1: The case of dimension $k = 1$ in ambient dimension $d = 2$ (the latter without loss of generality). What is pictured is in fact a piece of each curve. The reader is invited to imagine that these curves are completed by the same curve, say \mathcal{M}_0 , so that $\mathcal{M}_0 \cup \mathcal{M}_1$ and $\mathcal{M}_0 \cup \mathcal{M}_2$ are smooth simple closed curves. Also, additional points would be placed on \mathcal{M}_0 so that, together with the points depicted in the plot, they would form an ε -covering.

3.2.1 Case $k = 1$

As a warm-up, we consider the case where the underlying submanifold is a curve, meaning of dimension $k = 1$. It is enough to consider the plane ($d = 2$). There, let \mathcal{M}_1 be defined as the line segment $[0, 1] \times \{0\}$. Starting at the origin and moving right, place sample points ε apart, and assume for convenience that $\varepsilon = 1/(n - 1)$. The sample points are therefore $x_i = ((i - 1)\varepsilon, 0)$ for $i = 1, \dots, n$. We define \mathcal{M}_2 by bending and stretching \mathcal{M}_1 . To create an ‘arc’ between two sample points, we use a C^2 function w supported on $[-1, 1]$ and such that $w(0) = 1$. Define \mathcal{M}_2 by changing in \mathcal{M}_1 the line segment joining x_i and x_{i+1} into the curve given by the graph of the function $t \mapsto A(\varepsilon/2)^2 w((t - (i - 1/2)\varepsilon)/(\varepsilon/2))$ on the interval $[(i - 1)\varepsilon, i\varepsilon]$, doing so for each $i = 1, \dots, n$. Let $f_\varepsilon : [0, 1] \rightarrow \mathbb{R}$ denote the resulting function and $\gamma_\varepsilon(t) = (t, f_\varepsilon(t))$, and set $\mathcal{M}_2 = \gamma_\varepsilon([0, 1])$. By construction, \mathcal{M}_2 is a C^2 simple curve with curvature bounded from above by a universal constant multiple of A . The parameter $A > 0$ is fixed and only there to indicate that any upper bound on the curvature can be fulfilled by choosing A sufficiently small. The dependence on A is otherwise left implicit, as it is of secondary importance. See Figure 3.1 for an illustration.

Take $1 \leq i < j \leq n$. While the distance between x_i and x_j on \mathcal{M}_1 is obviously $(j - i)\varepsilon$, their distance on \mathcal{M}_2 is equal to the length of the piece of \mathcal{M}_2 starting at x_i and ending at x_j , which is equal to $(j - i)\eta$, where η is the length of the piece of \mathcal{M}_2 between x_1 and x_2 . Elementary calculations show that $\eta \geq \varepsilon + C_1\varepsilon^3$ for some $C_1 > 0$ which depends only on A . To be sure, assume that ε is small enough that $A(\varepsilon/2) \sup_t |w'(t)| \leq 1$, and compute

$$\begin{aligned} \eta &= \int_0^\varepsilon \left\{ 1 + [A(\varepsilon/2)^2 (2/\varepsilon) w'(2t/\varepsilon - 1)]^2 \right\}^{1/2} dt \\ &= \int_{-1}^1 \left\{ 1 + [A(\varepsilon/2) w'(t)]^2 \right\}^{1/2} (\varepsilon/2) dt \\ &\geq \int_{-1}^1 \left\{ 1 + \frac{1}{4} [A(\varepsilon/2) w'(t)]^2 \right\} (\varepsilon/2) dt = \varepsilon + C_1\varepsilon^3, \quad C_1 := \frac{1}{32} A^2 \int_{-1}^1 w'(t)^2 dt. \end{aligned}$$

Similar calculations show that $\eta \leq \varepsilon + C_2\varepsilon^3$, for another constant C_2 depending only on A . We have thus bounded η from below and above as follows

$$\varepsilon + C_1\varepsilon^3 \leq \eta \leq \varepsilon + C_2\varepsilon^3. \quad (3.2)$$

Using the lower bound in (3.2), we get that the distance on \mathcal{M}_2 between x_i and x_j is $\geq (j - i)(\varepsilon + C_1\varepsilon^3)$. In particular, because the distance on \mathcal{M}_1 between x_i and x_j is $= (j - i)\varepsilon$, when ε is sufficiently small, we have

$$d_{\mathcal{M}_2}(x_i, x_j) - d_{\mathcal{M}_1}(x_i, x_j) \geq (j - i)C_1\varepsilon^3 \geq C_1\varepsilon^2 d_{\mathcal{M}_1}(x_i, x_j).$$

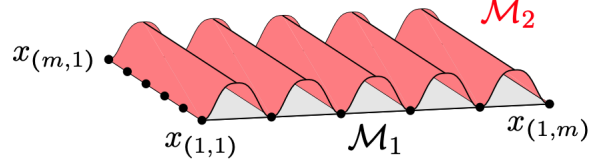


Figure 3.2: Analogous to Figure 3.1, but in the case of dimension $k = 2$ in ambient dimension $d = 3$.

Using the upper bound in (3.2), we get that

$$d_{\mathcal{M}_2}(x_i, x_j) - d_{\mathcal{M}_1}(x_i, x_j) \leq C_2 \varepsilon^2 d_{\mathcal{M}_1}(x_i, x_j) \leq d_{\mathcal{M}_1}(x_i, x_j),$$

with the last inequality holding as soon as ε is small enough that $C_2 \varepsilon^2 \leq 1$.

Based on what we know of the true \mathcal{M} , it could be \mathcal{M}_1 as easily as \mathcal{M}_2 , and therefore, for any estimate \hat{d}_{ij} ,

$$\begin{aligned} \max_{\mathcal{M} \in \{\mathcal{M}_1, \mathcal{M}_2\}} |\hat{d}_{ij} - d_{\mathcal{M}}(x_i, x_j)| &\geq \frac{1}{2} |d_{\mathcal{M}_2}(x_i, x_j) - d_{\mathcal{M}_1}(x_i, x_j)| \\ &\geq \frac{1}{4} C_1 \varepsilon^2 d_{\mathcal{M}_1}(x_i, x_j) \\ &\geq \frac{1}{8} C_1 \varepsilon^2 \max\{d_{\mathcal{M}_2}(x_i, x_j), d_{\mathcal{M}_1}(x_i, x_j)\} \\ &= \frac{1}{8} C_1 \varepsilon^2 \max_{\mathcal{M} \in \{\mathcal{M}_1, \mathcal{M}_2\}} d_{\mathcal{M}}(x_i, x_j). \end{aligned}$$

3.2.2 Case $k \geq 2$

In general, it is enough to consider the setting where $d = k + 1$. We also consider a regular grid where $x_i = (x_{i,1}, \dots, x_{i,k}, 0)$ with $i = (i_1, \dots, i_k)$ and $x_{i,q} = (i_q - 1)\varepsilon$ for $i_q = 1, \dots, m$ and $q = 1, \dots, k$. We are indeed assuming that n is of the form $n = m^k$ for some positive integer m . This is for convenience, although again, it brings the focus to what should in principle be a regular case (since the sample points are well spread out). We again assume for expediency that $\varepsilon = 1/(m - 1)$. We take $\mathcal{M}_1 = [0, 1]^k \times \{0\}$, and

$$\mathcal{M}_2 = \{(t_1, \dots, t_{k-1}, \gamma_\varepsilon(t_k)) : t_1, \dots, t_k \in [0, 1]\},$$

where γ_ε is the same parameterized curve that was constructed in Section 3.2.1. Clearly, the sample points belong to both surfaces. See Figure 3.2 for an illustration.

On the one hand, \mathcal{M}_1 is convex, and thus the intrinsic metric on \mathcal{M}_1 coincides with the Euclidean metric. In particular,

$$\begin{aligned} \text{dist}_{\mathcal{M}_1}(x_i, x_j)^2 &= \|x_i - x_j\|^2 \\ &= \sum_{q=1}^k (i_q - j_q)^2 \varepsilon^2, \end{aligned}$$

for all $i, j \in [m]^k$. On the other hand, recalling the definition of η given in Section 3.2.1, by straightening along the $(k + 1)$ th canonical direction, we see that \mathcal{M}_2 is isometric to $[0, 1]^{k-1} \times [0, (m - 1)\eta]$ via the isometry

$$(t_1, \dots, t_{k-1}, \gamma_\varepsilon(t_k)) \mapsto (t_1, \dots, t_{k-1}, \lambda_\varepsilon(t_k)),$$

where

$$\lambda_\varepsilon(t) := \Lambda(\gamma_\varepsilon([0, t])). \quad (3.3)$$

This isometry is based on an arc length parameterization of γ_ε . See Lemma 2.1. In particular, with this isometry

$$x_i \mapsto u_i := (x_{i,1}, \dots, x_{i,k-1}, \lambda_\varepsilon(x_{i,k})) = ((i_1 - 1)\varepsilon, \dots, (i_{k-1} - 1)\varepsilon, (i_k - 1)\eta).$$

As a consequence,

$$\begin{aligned} \text{dist}_{\mathcal{M}_2}(x_i, x_j)^2 &= \|u_i - u_j\|^2 \\ &= \sum_{q=1}^{k-1} (i_q - j_q)^2 \varepsilon^2 + (i_k - j_k)^2 \eta^2, \end{aligned}$$

for all $i, j \in [m]^k$. Hence,

$$\text{dist}_{\mathcal{M}_2}(x_i, x_j)^2 - \text{dist}_{\mathcal{M}_1}(x_i, x_j)^2 = (i_k - j_k)^2 (\eta^2 - \varepsilon^2),$$

and again, this is so for all $i, j \in [m]^k$. Using the upper bound in (3.2), if ε is sufficiently small that $C_2 \varepsilon^2 \leq 1$, we get

$$\begin{aligned} \text{dist}_{\mathcal{M}_2}(x_i, x_j)^2 - \text{dist}_{\mathcal{M}_1}(x_i, x_j)^2 &= (i_k - j_k)^2 (\eta - \varepsilon)(\eta + \varepsilon) \\ &\leq (i_k - j_k)^2 C_2 \varepsilon^3 (2\varepsilon + C_2 \varepsilon^3) \\ &\leq (i_k - j_k)^2 3C_2 \varepsilon^4 \\ &= 3C_2 \varepsilon^2 \beta_{ij}^2 \text{dist}_{\mathcal{M}_1}(x_i, x_j)^2 \\ &\leq 3 \text{dist}_{\mathcal{M}_1}(x_i, x_j)^2, \end{aligned}$$

where $\beta_{ij} := \cos(\theta_{ij})$ and θ_{ij} is the angle that the line passing through x_i and x_j makes with the k th axis. In the process, we found that

$$\text{dist}_{\mathcal{M}_2}(x_i, x_j) \leq 2 \text{dist}_{\mathcal{M}_1}(x_i, x_j).$$

From this, we get

$$\begin{aligned} \text{dist}_{\mathcal{M}_2}(x_i, x_j) - \text{dist}_{\mathcal{M}_1}(x_i, x_j) &\leq \frac{3C_2 \varepsilon^2 \beta_{ij}^2 \text{dist}_{\mathcal{M}_1}(x_i, x_j)^2}{\text{dist}_{\mathcal{M}_2}(x_i, x_j) + \text{dist}_{\mathcal{M}_1}(x_i, x_j)} \\ &\leq C_2 \varepsilon^2 \beta_{ij}^2 \text{dist}_{\mathcal{M}_1}(x_i, x_j). \end{aligned}$$

Using the lower bound in (3.2), we get

$$\begin{aligned} \text{dist}_{\mathcal{M}_2}(x_i, x_j)^2 - \text{dist}_{\mathcal{M}_1}(x_i, x_j)^2 &= (i_k - j_k)^2 (\eta - \varepsilon)(\eta + \varepsilon) \\ &\geq (i_k - j_k)^2 C_1 \varepsilon^4 \\ &= C_1 \varepsilon^2 \beta_{ij}^2 \text{dist}_{\mathcal{M}_1}(x_i, x_j)^2, \end{aligned}$$

and, as before, this implies that

$$\text{dist}_{\mathcal{M}_2}(x_i, x_j) - \text{dist}_{\mathcal{M}_1}(x_i, x_j) \geq \frac{1}{3} C_1 \varepsilon^2 \beta_{ij}^2 \text{dist}_{\mathcal{M}_1}(x_i, x_j).$$

Based on what we know of the true \mathcal{M} , it could be \mathcal{M}_1 as easily as \mathcal{M}_2 , and therefore, for any estimate \hat{d}_{ij} ,

$$\begin{aligned} \max_{\mathcal{M} \in \{\mathcal{M}_1, \mathcal{M}_2\}} |\hat{d}_{ij} - \mathbf{d}_{\mathcal{M}}(x_i, x_j)| &\geq \frac{1}{2} |\mathbf{d}_{\mathcal{M}_2}(x_i, x_j) - \mathbf{d}_{\mathcal{M}_1}(x_i, x_j)| \\ &\geq \frac{1}{6} C_1 \beta_{ij}^2 \varepsilon^2 \mathbf{d}_{\mathcal{M}_1}(x_i, x_j) \\ &\geq \frac{1}{12} C_1 \beta_{ij}^2 \varepsilon^2 \max\{\mathbf{d}_{\mathcal{M}_2}(x_i, x_j), \mathbf{d}_{\mathcal{M}_1}(x_i, x_j)\} \\ &= \frac{1}{12} C_1 \beta_{ij}^2 \varepsilon^2 \max_{\mathcal{M} \in \{\mathcal{M}_1, \mathcal{M}_2\}} \mathbf{d}_{\mathcal{M}}(x_i, x_j). \end{aligned}$$

We conclude with the fact that as $t \searrow 0$, the proportion of pairs (i, j) such that β_{ij}^2 exceeds t tends to 1.

4 Meshes

Polytopes form an important class of surfaces used in computational geometry, numerical partial differential equations, and more. Their approximation properties and their simplicity allow for the design of algorithms for rendering a surface on a computer under a chosen lighting condition, as done in 3D animation, or for simulating a particular equation arising in physics. Among polytopes that are routinely used in practice, simplicial complexes are arguably the most common. They are particularly relevant in our context as they are often used to assess the shape defined by an otherwise unorganized set of points. A finite collection K of simplexes constitutes a simplicial complex if it is closed under intersection (i.e., the intersection of two simplexes in K is either empty or itself a simplex of K) and if any face of a simplex in K is also a simplex in K .

When used to approximate of a surface, a simplicial complex is often called a mesh. A number of mesh construction are available in the literature, including some that come with theoretical guarantees — see Table 1 for some prominent examples. Because of the available theory, we work with the tangential Delaunay complex.

Table 1: Overview of some mesh constructions with their theoretical guarantees.

Method	Guarantees
Ball-pivoting [18, 36]	homeomorphism; watertight; bound in Hausdorff distance
Crust [5–8], Cocone [9]	homeomorphism; bound in Hausdorff distance and in angle
Tight Cocone [33, 34], Power Crust [10]	homeomorphism; watertight; bound in Hausdorff distance and in angle
Noisy Power Crust [34, 63]	homeomorphism
Natural Neighbors [20, 49]	homeomorphism; convergence in the Hausdorff metric
Peel [35]	isotopy; convergence in Hausdorff metric

4.1 Nets

The mesh construction we use — introduced in Section 4.2 below — requires that the data points form an ε -covering of \mathcal{M} , meaning that (1.1) holds, and that they form a $c\varepsilon$ -packing for some constant $c > 0$, meaning that

$$\min_{i \neq j} \|x_i - x_j\| \geq c\varepsilon.$$

Suppose we are interested in estimating $\mathbf{d}_{\mathcal{M}}(x_i, x_j)$ for a given pair of points indexed by $i, j \in [n]$. If $\|x_i - x_j\| \leq \varepsilon$, let the estimate be $\hat{d}_{ij} := \|x_i - x_j\|$.

Lemma 4.1 (Lem 3 in [19]; Lem 3.12 in [12]). *For \mathcal{M} satisfying Assumption 3.1, there is a constant C such that*

$$0 \leq \mathbf{d}_{\mathcal{M}}(x, x') - \|x - x'\| \leq C\|x - x'\|^3, \quad \forall x, x' \in \mathcal{M}.$$

Applying this lemma, we see that the bound in (1.4) applies for i, j , since

$$\begin{aligned} 0 \leq \mathbf{d}_{\mathcal{M}}(x_i, x_j) - \hat{d}_{ij} &\leq C\|x_i - x_j\|^3 \\ &\leq C\varepsilon^2 \hat{d}_{ij} \\ &\leq C\varepsilon^2 \min\{\mathbf{d}_{\mathcal{M}}(x_i, x_j), \hat{d}_{ij}\}, \end{aligned}$$

using the fact that $\hat{d}_{ij} = \|x_i - x_j\| \leq \varepsilon$.

If $\|x_i - x_j\| > \varepsilon$, do as follows. Starting with $S_0 := \{x_i, x_j\}$, at stage t , add a data point to S_t not within distance ε from a point in S_t to form S_{t+1} — stop at S_t if no such point exists. Let S_∞ denote the resulting subset of sample points. By construction, any two points in S_∞ are separated by a distance exceeding ε . Also, any sample point not included in S_∞ is within distance ε of a point in S_∞ , so that S_∞ is an 2ε -cover of \mathcal{M} by the triangle inequality. Following [21], S_∞ is an $(2\varepsilon, 1/2)$ -net of \mathcal{M} . (In general, a (η, c) -net of \mathcal{M} is a point set which is an η -covering of \mathcal{M} where any two points are at least $c\eta$ apart.) We then construct a mesh based on S_∞ and let \hat{d}_{ij} denote the distance on $\hat{\mathcal{M}}$ between x_i and x_j .

Therefore, in without loss of generality, in the remaining of this section, we simply assume that \mathbf{X} itself is an $(\varepsilon, 1/2)$ -net of \mathcal{M} .

Remark 4.2. Proceeding as a describe here would in principle require that we build a different mesh for each pair of points x_i and x_j such that $\|x_i - x_j\| > \varepsilon$. This would appear to be wasteful and unnecessary in practice. We believe this is indeed the case. See Section 6 for a longer discussion.

The construction below also requires that the sample points be in general position and that a certain ‘transversality’ condition⁵ be satisfied. If these conditions are not already satisfied, they can be achieved by a simple infinitesimal random perturbation of the sample points, and so we assume they are satisfied in what follows.

4.2 Tangential Delaunay complex

The tangential Delaunay complex is a mesh construction that dates back to [23, 42]. Here we follow the exposition given in [21, Ch 8]. In addition to the point set, $\{x_1, \dots, x_m\}$, the construction relies on knowledge of the tangent space at each sample point, meaning the knowledge of the tangent spaces at the sample points. We will see later in Section 4.3.1 that these tangent spaces can be estimated to enough precision to circumvent this otherwise substantial requirement.

Let \mathcal{U} denote the Delaunay complex of \mathbf{X} , which is the collection of all the simplexes with vertices in \mathbf{Y} that admit a circumscribing ball empty of sample points in its interior. For $i \in [n]$, let \mathcal{U}_i denote the Delaunay complex of \mathbf{X} restricted to the tangent space $T_i := T_{\mathcal{M}}(x_i)$, which is defined as the subcomplex of \mathcal{U} formed by all the simplexes that admit a circumscribing ball centered on T_i empty of sample points in its interior. The closed star of x_i in \mathcal{U}_i , denoted \mathcal{S}_i , is the subcomplex of \mathcal{U}_i that consists of the simplexes incident to x_i together with all their faces. With these definitions

⁵The condition is that no tangent space at any of the sample points contains a point that is equidistant to more than $k + 1$ points of \mathbf{X} .

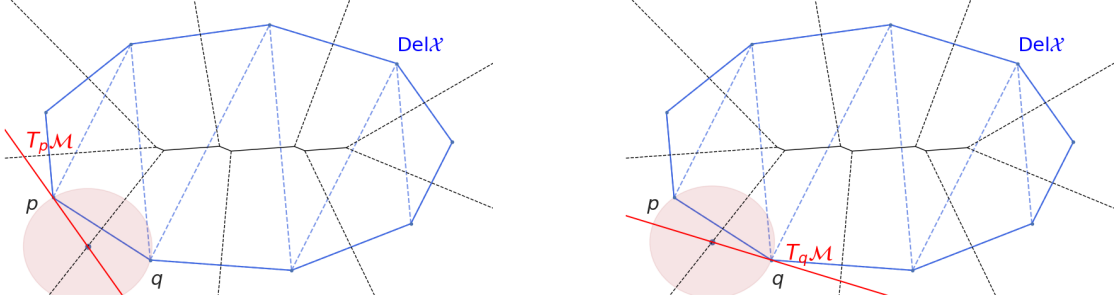


Figure 4.1: The Delaunay triangulation of a point cloud sampled from an ellipse is depicted in blue. The dual Voronoi diagram is in black. The edge $\sigma = \overline{pq}$ is a consistent simplex of the Tangential Delaunay complex because $\sigma \in \text{star}(p) \cap \text{star}(q)$. That is, σ can be circumscribed by empty balls centered on $T_p \mathcal{M}$ and $T_q \mathcal{M}$. (The balls, although very similar in this example, are not the same in general.)

in place, the tangential Delaunay complex of \mathbf{Y} is the simplicial complex made of the union of all these closed stars, i.e.,

$$\mathcal{T} := \{\sigma : \sigma \in \mathcal{S}_i \text{ for some } i \in [n]\}.$$

Because of the transversality condition mentioned above, \mathcal{T} does not contain faces of dimension greater than k .

When used to approximate a surface, the presence of thin simplexes or slivers (i.e., simplexes with small thickness as defined in Section 2.4) in a mesh can make restrict the accuracy of the approximation to the underlying surface to 0th order and be completely inaccurate at the level of the tangent spaces. This is due to the fact that slivers can make an arbitrarily large angle with the surface. In the extreme case, a sliver can even be perpendicular to the surface — think of three points along a same great circle on a 2D sphere. The Schwarz lantern provides a famous example of this: it is an arbitrarily fine mesh of a cylinder which converges in Hausdorff metric (i.e., 0th order) while the simplexes never become tangent to the cylinder in the infinitesimally fine mesh limit. In addition, thin simplexes can prevent the mesh from being a topological (in fact, piecewise linear) submanifold.

A simplex of the tangential Delaunay complex \mathcal{T} is said to be inconsistent if it does not belong to the closed stars of all of its vertices. In the presence of inconsistent simplexes, \mathcal{T} is not a topological submanifold. Without going into too much detail, to each inconsistent k -simplex of the tangential Delaunay complex, $\sigma \in \mathcal{T}$, we can associate a $(k+1)$ -simplex of the Delaunay complex, $\sigma^I \in \mathcal{U}$, that is said to ‘trigger’ the inconsistency; and, as it happens, that simplex σ^I cannot be too thick [21, Cor 8.13]. These inconsistencies are dealt with in [21] by perturbing \mathcal{U} using a variant of the weighing method of [29] which consists in lifting the points to dimension $d+1$ by assigning weights to them and then reassigning random weights (from a carefully chosen distribution) to the vertices of a sliver; see Algorithm 5 in [21]. The overall method for building a tangential Delaunay complex with no inconsistencies is described in Algorithm 8 in [21], and is shown to have expected running time proportional to the sample size [21, Th 8.17]. We refer to this algorithm as TDC. The overall algorithm is complex, but a relatively accessible although partial description is given in [2].

Theorem 4.3 (Th 7.16 and Th 8.18 in [21]). *There is a constant $C > 0$ depending on \mathcal{M} such*

that, if TDC is provided with an $(\varepsilon, 1/2)$ -net of \mathcal{M} together with the tangent spaces at each point of the net, then with probability 1 it returns a piecewise linear submanifold of dimension k without boundary that is a $C\varepsilon^2$ -distortion of \mathcal{M} .

We provide a sketch of a roadmap through the book of Boissonnat *et al* [21] that leads to the result. Let \mathcal{T}_c denote the output of TDC, that is, the tangential Delaunay complex built on the provided sample of points together with the accompanying tangents spaces — corrected for inconsistencies. According to [21, Th 8.18] the simplexes of \mathcal{T}_c all have thickness at least $1/C_0$, and \mathcal{T}_c and \mathcal{M} are within Hausdorff distance $C_0\varepsilon^2$. The proof of that result consists in large part in verifying that the conditions of [21, Th 7.16] are satisfied, which in particular includes showing that the simplexes of \mathcal{T}_c all have diameter at most $C_0\varepsilon$ and also that the projection map $P_{\mathcal{M}} : \mathcal{T}_c \rightarrow \mathcal{M}$ (which is well-defined when $C_0\varepsilon^2 < \rho(\mathcal{M})$, which we assume is the case) is one-to-one. To complete the picture, the projection map is shown to be a $O(\varepsilon^2)$ -distortion map. By [21, Lem 7.13] (or our Lemma 2.4), this is true on each simplex of \mathcal{T}_c by the above bounds on the thickness and diameter, and thus true on the entirety of \mathcal{T}_c seen as a surface.

4.3 Estimation of the tangential Delaunay complex

We just saw that the tangential Delaunay complex, after correction for inconsistencies, provides a good enough approximation to the underlying surface for the metric approximation (1.4) to hold. In addition, from an algorithmic standpoint, the complex can be built in (randomized) polynomial time, and results in a piecewise linear surface for which algorithms for computing distances exist (see Section 4.4). All that said, the construction relies on knowing the tangent spaces at the sample points, which in principle is not part of the information we have access to.

As it turns out, this additional information is not needed: In the same setting, the tangent spaces can be estimated to enough accuracy that the construction of the tangential Delaunay complex based on these estimated tangent spaces, again after correction for inconsistencies, also provides a good enough approximation to the underlying surface. All we need is a lower bound on the reach of \mathcal{M} — a more reasonable requirement.

The same strategy is considered by Aamari and Levrard [2]. We follow in their footsteps to obtain the desired bound on the distortion between the estimated tangential Delaunay complex and the underlying surface.

4.3.1 Estimating the tangent spaces

The estimation of tangent spaces is by local principal component analysis, a natural approach used throughout the manifold estimation literature and manifold learning literature (e.g., in [13, 43, 52, 83]). While [2] works with a random sample, we show below that the same accuracy results if we work instead with an $(\varepsilon, 1/2)$ -net as we do here.

Let \hat{T}_i denote the k -dimensional affine space that passes through x_i and is parallel to the top k -dimensional eigenspace of the following matrix

$$\Sigma_i := \frac{1}{|N_i|} \sum_{j \in N_i} (x_j - x_i)(x_j - x_i)^\top, \quad N_i := \{j \in [n] : \|x_j - x_i\| \leq h\}. \quad (4.1)$$

That eigenspace will be shown to be well-defined when h is chosen proportional to ε and ε is small enough. Unlike [2], this matrix is not the covariance matrix of the sample points in $B(x_i, h)$ as it is centered at x_i and not at the barycenter of those points. This is not essential, but helps streamline the proof of the following result.

Below, we will use \leq to denote the Loewner order when comparing symmetric matrices of same size. For a symmetric matrix M , $\lambda_1(M) \geq \lambda_2(M) \geq \dots$ denote its eigenvalues thus ordered.

Proposition 4.4. *Choose $h = A\varepsilon$ in (4.1) for a constant A depending only on k specified below. There is $C > 0$ depending only on \mathcal{M} such that $\angle(\hat{T}_i, T_i) \leq C\varepsilon$ for all i .*

Proof. In what follows, $A = 3/\eta_0$ where η_0 is implicitly defined in Lemma 4.5. We only need to prove the statement for ε sufficiently small because an angle is bounded.

Let P_i be short for P_{T_i} . Let t_j denote the orthogonal projection of x_j onto T_i . First, note that $t_i = x_i$, and for $j \in N_i$,

$$\|t_j - x_j\| = \text{dist}(x_j, T_i) \leq C_1 \|x_j - x_i\|^2 \leq C_1 h^2,$$

by Lemma 2.10, so that

$$\|t_j - t_{j'}\| \geq \|x_j - x_{j'}\| - \|t_j - x_j\| - \|t_{j'} - x_{j'}\| \geq \varepsilon/2 - C_1 h^2 - C_1 h^2,$$

by the triangle inequality.

Next, we claim that $\{t_j : j \in N_i\}$ forms an $(\varepsilon + C_2 h^3)$ -covering of $B(x_i, h) \cap T_i$, where C_2 is the constant of Lemma 2.11. Indeed, take $t \in B(x_i, h) \cap T_i$ and let $t' \in B(x_i, h - C_2 h^3) \cap T_i$ be such that $\|t' - t\| \leq C_2 h^3$. By Lemma 2.11, there is $x' \in B(x_i, h) \cap \mathcal{M}$ such that $P_i(x') = t'$. Since $\{x_j : j \in N_i\}$ is an ε -covering of $B(x_i, h - \varepsilon) \cap \mathcal{M}$, there must be $j \in N_i$ be such that $\|x_j - x'\| \leq \varepsilon$. Then $\|t_j - t'\| \leq \varepsilon$ because P_i is 1-Lipschitz. By the triangle inequality, we get $\|t_j - t\| \leq \varepsilon + C_2 h^3$. Note that, for any $j \in N_i$, $t_j \in B(x_i, h) \cap T_i$, since $\|t_j - t_i\| \leq \|x_j - x_i\| \leq h$, again relying on P_i being 1-Lipschitz. Hence, recalling that $h = A\varepsilon$, if ε is small enough that

$$\varepsilon/2 - 2C_1(A\varepsilon)^2 > \varepsilon/3 \quad \text{and} \quad \varepsilon + C_2(A\varepsilon)^3 \leq 2\varepsilon,$$

we have that $\{t_j : j \in N_i\}$ forms a $(2\varepsilon, 1/6)$ -net of $B(x_i, h) \cap T_i$.

Now, remembering that $t_i = x_i$, we have

$$\Sigma_i = \Sigma_i^{\text{proj}} + R_1 + R_1^\top + R_2, \quad \text{with} \quad \Sigma_i^{\text{proj}} := \frac{1}{|N_i|} \sum_{j \in N_i} (t_j - t_i)(t_j - t_i)^\top,$$

and remainders

$$R_1 := \frac{1}{|N_i|} \sum_{j \in N_i} (x_j - t_j)(t_j - t_i)^\top, \quad R_2 := \frac{1}{|N_i|} \sum_{j \in N_i} (x_j - t_j)(x_j - t_j)^\top.$$

satisfying

$$\|R_1\| \leq \max_{j \in N_i} \|x_j - t_j\| \|t_j - t_i\| \leq (C_1 h^2) h = C_1 h^3,$$

$$\|R_2\| \leq \max_{j \in N_i} \|x_j - t_j\|^2 \leq (C_1 h^2)^2 = C_3 h^4.$$

Hence,

$$\|\Sigma_i - \Sigma_i^{\text{proj}}\| \leq C_1 h^3 + C_1 h^3 + C_3 h^4 \leq C_4 h^3,$$

assuming ε is small enough that $h = A\varepsilon \leq 1$. By rescaling the t_j and applying Lemma 4.5 below (A was chosen to make things work), we find that

$$C_5^{-1} h^2 P_i \leq \Sigma_i^{\text{proj}} \leq C_5 h^2 P_i.$$

When this is the case, Σ_i^{proj} has exactly k nonzero eigenvalues, all between $C_5^{-1}h^2$ and C_5h^2 , and so by the Davis–Kahan $\sin \Theta$ theorem [76, Th V.3.6],

$$\|Q_i - Q_i^{\text{proj}}\| \leq \frac{\sqrt{2} \|\Sigma_i - \Sigma_i^{\text{proj}}\|}{\lambda_k(\Sigma_i^{\text{proj}}) - \lambda_{k+1}(\Sigma_i^{\text{proj}})} \leq \frac{\sqrt{2} C_4 h^3}{C_5^{-1} h^2} = C_6 h,$$

where Q_i and Q_i^{proj} are the projections onto the top k -dimensional eigenspaces of Σ_i and Σ_i^{proj} respectively. Since $Q_i^{\text{proj}} = P_i$, the result follows from Lemma 2.9 and the fact that $\sin a \geq \frac{2}{\pi} a$ for all $a \in [0, \frac{\pi}{2}]$. \square

Lemma 4.5. *Suppose that $u_1, \dots, u_N \in \mathbb{R}^k$ is a $(\eta, 1/C_1)$ -net of the unit ball. Define $\Sigma = \frac{1}{N} \sum_j u_j u_j^\top$. Then, for $\eta \leq \eta_0$ for some $\eta_0 > 0$ depending only on k and $C_2 \geq 1$ depending only on k and C_1 , we have $C_2^{-1} \mathbf{I} \leq \Sigma \leq C_2 \mathbf{I}$.*

Proof. Let B_0 denote the unit ball in \mathbb{R}^k . We make use of Riemann sums. Let V_j denote the cell corresponding to u_j in the Voronoi partition of B_0 based on u_1, \dots, u_N , and define

$$\tilde{\Sigma} := \sum_{j \in [N]} \mu(V_j) u_j u_j^\top.$$

Using the fact that $u \mapsto uu^\top$ is 2-Lipschitz on B_0 , we have

$$\left\| \tilde{\Sigma} - \int_{B_0} uu^\top du \right\| \leq 2 \max_{j \in [N]} \text{diam}(V_j), \quad (4.2)$$

where μ denotes the Lebesgue measure.

We now show that $\mu(V_j)$ is of order η^k uniformly in j . Indeed, on the one hand, $\|u_j - u_l\| > \eta/C_1$, so that $B(u_j, \eta/2C_1) \subset V_j$, implying that

$$\mu(V_j) \geq \mu(B(u_j, \eta/2C_1)) \geq \mu(B_0)(\eta/2C_1)^k =: \eta^k/C_3.$$

On the other hand, $V_j \subset B(u_j, 2\eta)$ since any $u \in B_0$ such that $\|u - u_j\| > \eta$ must be within η of some u_l other than u_j , and this implies that

$$\mu(V_j) \leq \mu(B(u_j, 2\eta)) \leq \mu(B_0)(2\eta)^k =: C_4 \eta^k.$$

Because $\sum_j \mu(V_j) = \mu(B_0) = 1$ and $N \min_j \mu(V_j) \leq \sum_j \mu(V_j) \leq N \max_j \mu(V_j)$, all this implies that $\eta^{-k}/C_4 \leq N \leq C_3 \eta^{-k}$. We thus have

$$(C_3 C_4)^{-1} \Sigma \leq N (\min_j \mu(V_j)) \Sigma \leq \tilde{\Sigma} \leq N (\max_j \mu(V_j)) \Sigma \leq (C_3 C_4) \Sigma.$$

Reorganized, this gives

$$(C_3 C_4)^{-1} \tilde{\Sigma} \leq \Sigma \leq (C_3 C_4) \tilde{\Sigma}.$$

Note that C_3 and C_4 only depend on k and C_1 .

Along the way, we also found that $\text{diam}(V_j) \leq 4\eta$ due to $V_j \subset B(u_j, 2\eta)$. And since, by symmetry,

$$\int_{B_0} yy^\top dy = C_5 \mathbf{I},$$

for C_5 depending only on k , going back to (4.2), we find that the eigenvalues of $\tilde{\Sigma}$ are between $C_5 - 8\eta$ and $C_5 + 8\eta$. Let $\eta_0 = C_5/16$, defined so that $C_5 - 8\eta_0 \geq C_5/2$ and $C_5 + 8\eta_0 \leq 2C_5$. Then, for $\eta \leq \eta_0$, the eigenvalues of Σ are between $C_5/(2C_3 C_4)$ and $(2C_3 C_4)C_5$. \square

4.3.2 Estimating the surface

Having estimated the tangent space T_i at each point $x_i \in \mathbf{X}$, resulting in \hat{T}_i , we build the tangential Delaunay complex (corrected for inconsistencies), denoted $\hat{\mathcal{T}}_c$.

The proof of Theorem 4.7 relies on a result borrowed⁶ from [2], which in words says that if the estimates for the tangent spaces are accurate enough then there is a surface with positive reach which also passes through the sample points and for which each estimated tangent space corresponds to its actual tangent space at the corresponding location.

Proposition 4.6 (Th 4.1 in [2]). *In the present context, suppose that, for all $i \in [n]$, \tilde{T}_i is a k -dimensional affine subspace passing through x_i such that $\angle(T_i, \tilde{T}_i) \leq \theta$. There is a constant C depending on \mathcal{M} such that, if $\varepsilon \leq 1/C$ and $\theta \leq 1/C$, then there is a surface $\tilde{\mathcal{M}}$ satisfying Assumption 3.1 with reach $\geq 1/C$ and within Hausdorff distance $C\theta\varepsilon$ from \mathcal{M} such that $x_i \in \tilde{\mathcal{M}}$ and $T_{\tilde{\mathcal{M}}}(x_i) = \tilde{T}_i$ for all $i \in [n]$.*

In its original statement, [2, Th 4.1] also says that \mathcal{M} and $\tilde{\mathcal{M}}$ are diffeomorphic, and in fact, a look at the proof of that result, in particular from [2, Lem 4.2], reveals that they are $O(\varepsilon)$ distortions of each other. This is not quite enough for our purposes, and therefore we do not use this part of the result. See Section 6 for a longer discussion.

4.3.3 Estimating the distances

With $\hat{\mathcal{T}}_c$ at our disposal, we compute the pairwise distances on $\hat{\mathcal{T}}_c$ to obtain

$$\hat{d}_{ij} := d_{\hat{\mathcal{T}}_c}(x_i, x_j), \quad i, j \in [n]. \quad (4.3)$$

Theorem 4.7. *There is $C > 0$ depending only on \mathcal{M} such that, if $\varepsilon \leq 1/C$, then the estimator (4.3) satisfies (1.4).*

Proof of Theorem 4.7. First, let C_0 denote the constant of Proposition 4.4 and let C_1 be the constant of Proposition 4.6. Suppose ε is small enough that $C_0\varepsilon \leq 1/C_1$, so that Proposition 4.6 applies to yield the existence of a surface $\tilde{\mathcal{M}}$ satisfying Assumption 3.1 such that: it contains the sample points \mathbf{X} ; its tangent spaces at the sample points coincide with the estimated tangent spaces, i.e., $T_{\tilde{\mathcal{M}}}(x_i) = \tilde{T}_i$ for all $i \in [n]$; it has reach $\geq 1/C_1$; and it is within Hausdorff distance $C_1\varepsilon^2$. By Lemma 2.5, we have

$$|d_{\mathcal{M}}(x_i, x_j) - d_{\tilde{\mathcal{M}}}(x_i, x_j)| \leq C_2\varepsilon^2 d_{\mathcal{M}}(x_i, x_j), \quad \forall i, j \in [n].$$

Next, suppose ε is small enough that Theorem 4.3 applies, so that $\hat{\mathcal{T}}_c$ and the surface $\tilde{\mathcal{M}}$ are in one-to-one correspondence via a $C_3\varepsilon^2$ -distortion map. By Corollary 2.3, this implies that

$$|d_{\tilde{\mathcal{M}}}(x_i, x_j) - d_{\hat{\mathcal{T}}_c}(x_i, x_j)| \leq C_4\varepsilon^2 d_{\hat{\mathcal{T}}_c}(x_i, x_j), \quad \forall i, j \in [n].$$

Combining these two bounds using the triangle inequality, we get for any pair $i, j \in [n]$,

$$|d_{\mathcal{M}}(x_i, x_j) - d_{\hat{\mathcal{T}}_c}(x_i, x_j)| \leq C_5\varepsilon^2 (d_{\mathcal{M}}(x_i, x_j) + d_{\hat{\mathcal{T}}_c}(x_i, x_j)),$$

and, if ε is small enough that $C_5\varepsilon^2 \leq 1/3$, this implies that

$$|d_{\mathcal{M}}(x_i, x_j) - d_{\hat{\mathcal{T}}_c}(x_i, x_j)| \leq C_6\varepsilon^2 \min\{d_{\mathcal{M}}(x_i, x_j), d_{\hat{\mathcal{T}}_c}(x_i, x_j)\},$$

which gives the desired bound. \square

⁶The lower bound on the reach stated in Th 4.1 in [2] appears incorrect. We followed the arguments backing that result, especially Lem 4.2, to arrive at the lower bound on the reach given here.

4.4 Numerical experiments

We performed some numerical experiments to illustrate our theory. We focused on the most interesting case accessible to computations, that of points on a $(k = 2)$ -dimensional surface embedded in a Euclidean space of dimension $d = 3$. We chose to work with such emblematic surfaces as the sphere, the torus, and the Swiss roll (even though the latter has a boundary).

4.4.1 Data

Armed with a parameterization of a surface, we generate sample points by drawing from the uniform distribution on the parameter domain independently n times, n being the desired sample size (which varies in our experiments). We then subsampled the points to obtain a net. For simplicity, this subset of points was considered to be the entire sample.

These are the parameterizations that we used:

$$\begin{aligned} \text{sphere:} \quad & (u, v) \in [0, 2\pi) \times [0, \pi) \mapsto (\cos(u) \cos(v), \sin(u) \cos(v), \sin(v)); \\ \text{torus:} \quad & (u, v) \in [0, 2\pi) \times [0, 2\pi) \mapsto (\cos(u)(2 + \cos v), \sin(u)(2 + \cos v), \sin v); \\ \text{Swiss roll:} \quad & (u, v) \in [\pi/4, 9\pi/4] \times [0, 1] \mapsto (u \cos u, u \sin u, v). \end{aligned}$$

4.4.2 Mesh construction

The generation a mesh from the point cloud, specifically, the tangential Delaunay complex, was done via the implementation available in the *Geometry Understanding in Higher Dimensions (GUDHI)* library [50]. The main parameters are the maximum perturbation radius, which is a constraint on the amount that points may be perturbed in an effort to reduce inconsistencies, and the maximum squared edge length of a simplex. With a dataset that has undergone preprocessing to yield a net, the parameter values do not significantly alter the resulting mesh. The maximum squared edge length is the most crucial parameter to adjust when some areas of the surface are poorly sampled. It was set using a priori knowledge of the true underlying surface.

In Figure 4.2, we provide examples of tangential Delaunay complex mesh constructions for the sphere, the torus, and the Swiss roll, and do so for various sample sizes.

4.4.3 Shortest paths

We now turn to evaluating the accuracy of the proposed method for estimating the pairwise distances on a surface. As benchmark, we use Isomap [78]. Isomap estimates pairwise distances on the underlying surface by forming a neighborhood graph and then computing the shortest-path distances using Dijkstra’s algorithm.⁷ The accuracy of this estimation depends crucially on the connectivity radius $r > 0$ which defines the neighborhood graph. As there is no standard data-driven way to choose this connectivity radius, in our experiment, we look at various choices in a reasonable range.

On the other hand, after meshing — which, it is true, may require some tuning to achieve a reasonable reconstruction — computing distances on the mesh does not require further tuning. In our experiments, we used the the ‘triangulated surface mesh shortest paths’ module of the *Computational Geometric Algorithms Library (CGAL)*, which implements a variation of the Chen–Han algorithm [28, 54, 85].

⁷The igraph package was used to compute shortest paths on graphs [31].

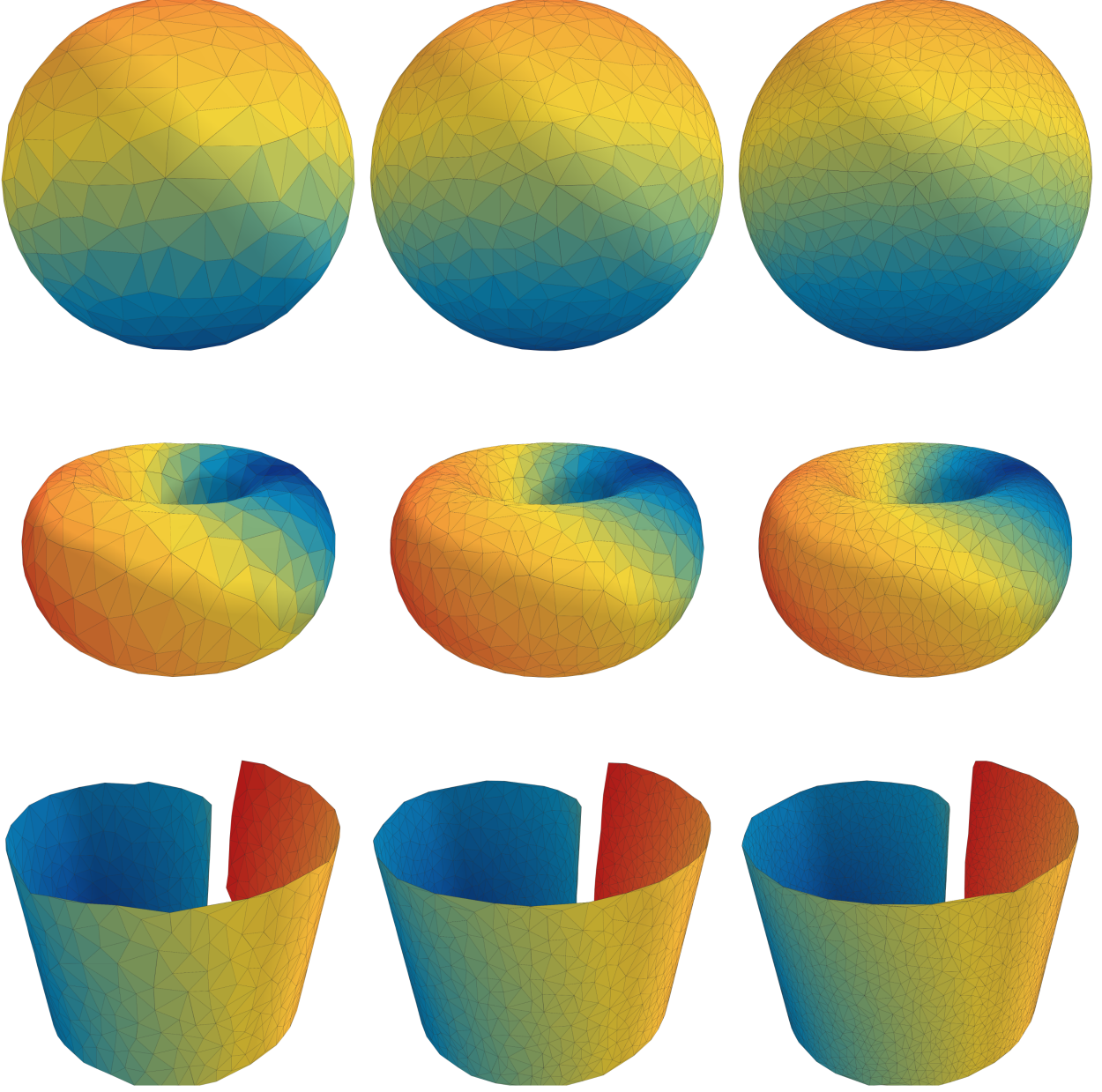


Figure 4.2: Examples of tangential Delaunay complex mesh constructions on the sphere, the torus, and the Swiss roll (top to bottom) based on uniform samples of size 500, 1000, and 2000 (left to right). The color signifies the distance to a fixed source point, from closer (blue) to farther (red).

For the sphere \mathbb{S}^2 , the great circle distance (i.e., intrinsic distance) is given by $\cos^{-1}\langle x, y \rangle$ between $x, y \in \mathbb{S}^2$. The Swiss roll is another nice surface to work with because there is a global isometry between the surface and a rectangle in \mathbb{R}^2 . Let $\gamma(t) = (\gamma_1(t), \gamma_2(t)) := (t \cos(\alpha t), t \sin(\alpha t))$. The arc length is given by

$$s(t) = \int_0^t \|\dot{\gamma}(t)\| dt = \int_0^t \left[\frac{t}{2} \sqrt{1 + (\alpha t)^2} + \frac{1}{2\alpha} \sinh^{-1}(\alpha t) \right] dt.$$

The inverse $t = t(s)$ is calculated with Newton's method. By construction, $\phi(s, z) := (\gamma_1(s), \gamma_2(s), z)$

is an isometry, and in particular,

$$d_{\mathcal{M}}(\phi(s_1, z_1), \phi(s_2, z_2)) = \sqrt{(s_1 - s_2)^2 + (z_1 - z_2)^2}.$$

By contrast, the torus is not as easy to handle. It does admit a C^1 isometry into \mathbb{R}^3 , but not a C^2 isometry, and the C^1 isometry is rather complex [26]. We opted for a numerical approximation ascertained by the use of a midpoint method initialized with the output from a neighborhood graph distances. The method is iterative. From an existing approximating path, say $\gamma^{(t)}$ at iteration t , a new path is constructed at iteration $t + 1$ by first splitting each line segment of $\gamma^{(t)}$ in half and then projecting the resulting piecewise linear path back onto the surface. The results of these experiments are reported in Figure 4.3 (sphere), Figure 4.4 (torus), and Figure 4.5 (Swiss roll). For the sphere and Swiss roll, mesh distances are noticeably more accurate on average than graph distances, and so across a wide range of choices of the connectivity radius of the graph. For the torus, the mesh distances are only slightly better than graph distances corresponding to the best choice of connectivity radius. (We again note that the choice of radius is typically done in a rather ad hoc manner in practice.)

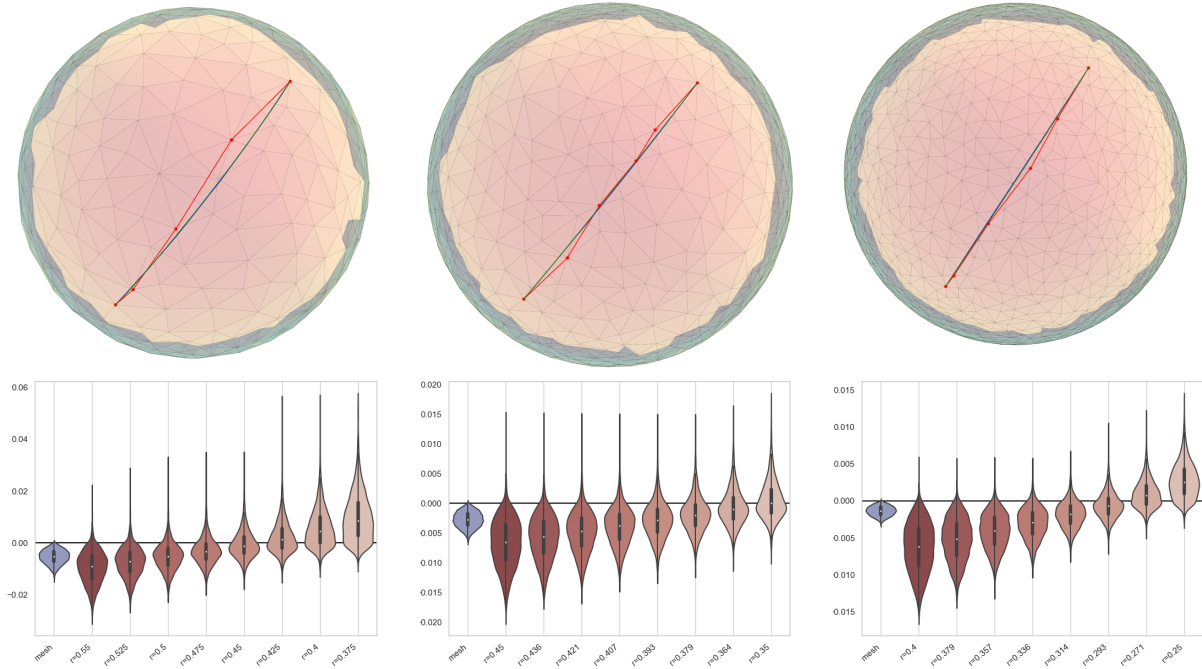


Figure 4.3: Estimation of distances for the sphere. Sample size $n = 500, 1000, 2000$ (left to right). Top row: Examples of computed shortest paths comparing the true path (green), path computed on the mesh (blue), and a typical path computed on the neighborhood graph (red). The first two paths almost overlap. Bottom row: Signed error (estimate - true) averaged over 50 repeats for the distance computed on the mesh and for the distance computed on a neighborhood graph of varying connectivity radius r .

We also examined the accuracy of the two methods as a function of the sample size. For this experiment, we focused on the sphere. As we explored larger sample sizes, we approximate the error by evaluating the difference between true and estimated distance on 100 pairs of points chosen at random. The result of this experiment is reported in Figure 4.6.

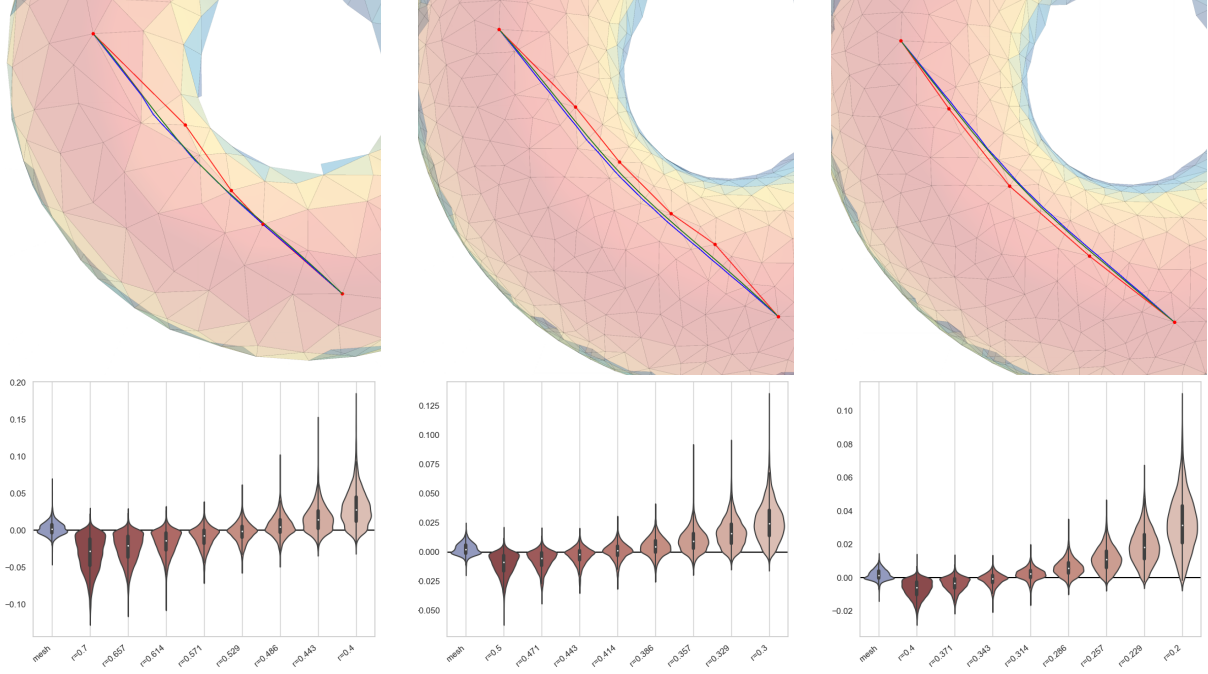


Figure 4.4: Estimation of distances for the torus. (See Figure 4.3 for details.)

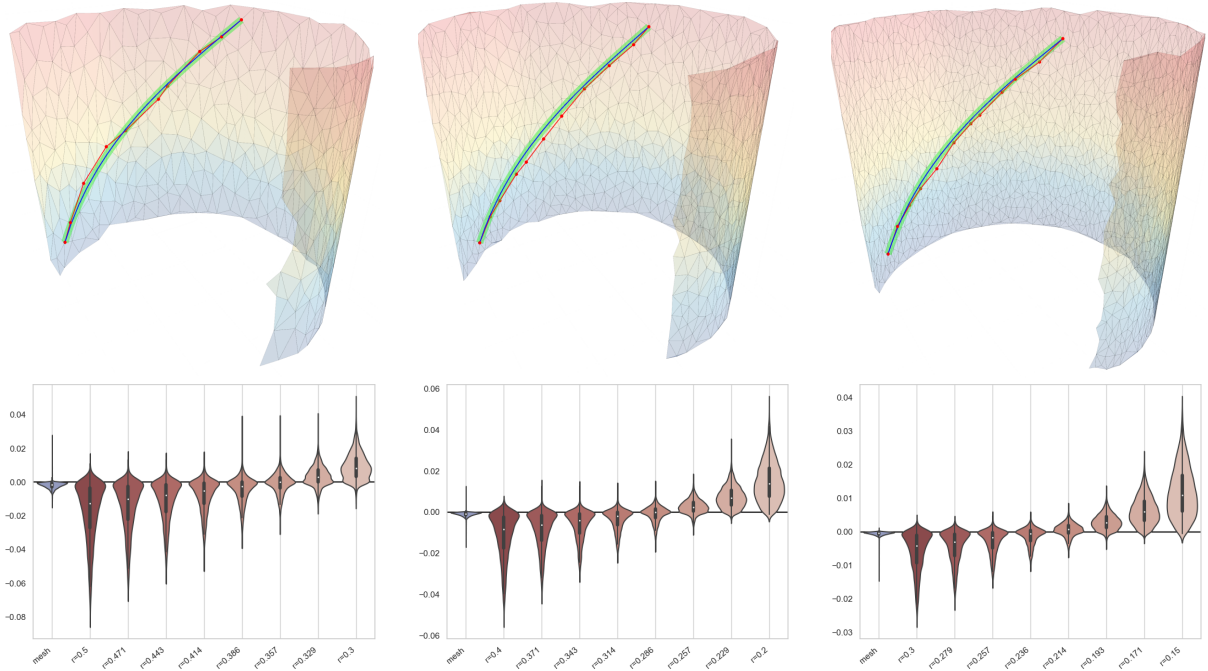


Figure 4.5: Estimation of distances for the Swiss roll. (See Figure 4.3 for details.)

5 Minimax manifold learning

The modern era of manifold learning, aka (nonlinear) dimensionality reduction, may have started with the advent of Isomap [77, 78] and Local Linear Embedding (LLE) [68]. This led to a flurry of methods, including Laplacian Eigenmaps [16], Manifold Charting [27], Diffusion Maps [30],

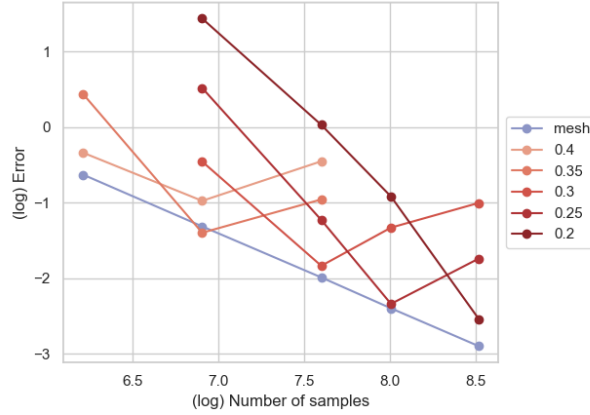


Figure 4.6: Estimation of distances on the sphere. The setting is as in Figure 4.3, except that here we look at a wider range of sample sizes. (Also, the error is absolute, not signed.) The values of the neighborhood radius — each with a different color specified in the side legend box — were chosen so as to optimize the accuracy of corresponding distance estimation.

Hessian Eigenmaps (HLE) [38], Local Tangent Space Alignment (LTSA) [88], Maximum Variance Unfolding (aka Semidefinite Embedding) [82], t -SNE [61], and UMAP [62], among others.

Some theory was developed for many of them, in the original article or in followup publications such as [11, 14, 17, 19, 45, 46, 48, 74, 75, 81, 86, 87]. To this day, however, there is no optimality theory of manifold learning — at least as far as we know. In fact, there is no clear agreement on what manifold learning is all about. We focus here on what we believe to be the simplest, and arguably the most fundamental framework for manifold learning: recovering a global isometry when one exists. Thus we assume that the underlying surface $\mathcal{M} \subset \mathbb{R}^d$ is isometric to a (compact) domain $\mathcal{U} \subset \mathbb{R}^k$ of full dimension (i.e., with non-empty interior). If $\phi : \mathcal{U} \rightarrow \mathcal{M}$ is such an isometry, then the goal is to estimate the embedded points $u_i := \phi^{-1}(x_i)$, up to a rigid transformation. Remember that $\mathbf{X} = \{x_1, \dots, x_n\}$ denotes the sample and is assumed to belong to \mathcal{M} . We denote $\mathbf{U} := \{u_1, \dots, u_n\}$. Note that, because of the isometric correspondence, since \mathbf{X} is an ε -covering of \mathcal{M} , \mathbf{U} is an ε -covering of \mathcal{U} .

Because the domain \mathcal{U} has a boundary, so does \mathcal{M} . To keep the exposition simple, and to enable Isomap and the variant we propose to be consistent, we assume that \mathcal{U} is convex. To be specific, we assume the following.

Assumption 5.1. There is a compact and convex domain with non-empty interior in \mathbb{R}^k and a C^2 isometry defined on an open set containing that domain such that \mathcal{M} is the image of that domain via that isometry.

In our context, two embeddings are necessarily compared up to a rigid transformation. We are able to leverage the results from Section 3 to establish the existence of an embedding procedure that returns $\hat{u}_1, \dots, \hat{u}_n$ with error bounded as follows

$$\min_{Q \in \mathbb{Q}_k} \max_{i \in [n]} \|\hat{u}_i - Q(u_i)\| \leq C\varepsilon^2, \quad (5.1)$$

where \mathbb{Q}_k denotes the class of rigid transformations of \mathbb{R}^k , and C is a constant that depends on \mathcal{M} .

5.1 Embedding by surface reconstruction

As we noted in Remark 3.6, the derivations and conclusions of Section 3.1 can be extended to surfaces with ‘nice-enough’ boundary, which is certainly the case for surfaces that satisfy Assumption 5.1. Following what we did in that section, let $\mathbb{M} = \mathbb{M}(k, \mathbf{X}, \varepsilon)$ denote the class of surfaces satisfying Assumption 5.1 for which \mathbf{X} is an ε -covering. We know that \mathbb{M} is non-empty since $\mathcal{M} \in \mathbb{M}$. Let ρ_{\max} denote the supremum reach among surfaces in \mathbb{M} , and let α_{\max} denote the maximum α (defined in Remark 3.6) of a surface in \mathbb{M} with $\text{reach} \geq \rho_{\max}/2$. Finally, select any surface $\hat{\mathcal{M}} \in \mathbb{M}$ satisfying $\rho(\hat{\mathcal{M}}) \geq \rho_{\max}/2$ and $\alpha(\hat{\mathcal{M}}) \geq \alpha_{\max}/2$. (As before, what matters is that the regularity of $\hat{\mathcal{M}}$ is controlled as a function of \mathcal{M} .)

With the interpolating surface $\hat{\mathcal{M}}$ defined, we have two choices:

- Because $\hat{\mathcal{M}}$ is in the class \mathbb{M} , it comes⁸ with a compact and convex domain with non-empty interior in \mathbb{R}^k , say $\hat{\mathcal{U}}$, and a C^2 isometry defined on an open set containing $\hat{\mathcal{U}}$ such that $\hat{\phi}(\hat{\mathcal{U}}) = \hat{\mathcal{M}}$. By applying the inverse of this isometry to the data points, we obtain an embedding in \mathbb{R}^k given by

$$\hat{u}_1 := \hat{\phi}^{-1}(x_1), \dots, \hat{u}_n := \hat{\phi}^{-1}(x_n). \quad (5.2)$$

- We estimate the metric on \mathcal{M} by the metric on $\hat{\mathcal{M}}$ as done in (3.1) and then apply Classical Scaling to the set of estimated distances $(d_{\hat{\mathcal{M}}}(x_i, x_j))$ to get an embedding, $\hat{u}_1, \dots, \hat{u}_n \in \mathbb{R}^k$.

The second option is seemingly more constructive, but it builds on the selection of $\hat{\mathcal{M}}$, which is non-constructive. As it turns out, the two options give the same embedding (up to a rigid transformation). This is so because

$$\hat{d}_{ij} = d_{\hat{\mathcal{M}}}(x_i, x_j) = \|\hat{\phi}^{-1}(x_i) - \hat{\phi}^{-1}(x_j)\|,$$

so that $\hat{\phi}^{-1}(x_1), \dots, \hat{\phi}^{-1}(x_n)$ is a perfect realization of (\hat{d}_{ij}) into \mathbb{R}^k and it is well-known that Classical Scaling returns a perfect realization when one exists.

Theorem 5.2. *There is a constant $C > 0$ depending on \mathcal{M} such that, if $\varepsilon \leq 1/C$, the embedding (5.2) satisfies the error bound (5.1).*

We used Classical Scaling above as this is the method used in the main Isomap variant [78], but many other methods for MDS are available. For technical reasons which we explain later on, we use a landmark variant of Classical Scaling. This method was proposed by some of the same others [32, 73] as a speedup of Classical Scaling. It consists in 1) selecting a few items; 2) embedding these items by Classical Scaling; 3) embedding the other items by lateration by reference to the points obtained in Step 2. Lateration consists in locating a point based on its distance to known ‘landmark’ points. The lateration method used in [32, 73] was first proposed by Gower [47]. It is known that, just like Classical Scaling, landmark Classical Scaling returns a perfect realization when one exists as long as the landmark items are chosen in Step 1 correspond to points that span the entire Euclidean space where the embedding takes place. Therefore, applying Classical Scaling or its landmark variant to $(d_{\hat{\mathcal{M}}}(x_i, x_j))$, we obtain an embedding of the form (5.2) in either case. For reference, Classical Scaling is Algorithm 2 and Gower’s lateration is Algorithm 3 in [11].

The technical reason why we use landmark Classical Scaling below is because of the perturbation bounds available to us. For $y_1, \dots, y_m \in \mathbb{R}^k$ and $\mathbf{Y} := \{y_1, \dots, y_m\}$, simultaneously seeing as an $n \times k$ matrix with row vectors y_i , define

$$\text{diam}_2(\mathbf{Y}) = 2\|\mathbf{Y}\|/\sqrt{m}, \quad \text{width}_2(\mathbf{Y}) = 2\|\mathbf{Y}^\dagger\|^{-1}/\sqrt{m}, \quad (5.3)$$

⁸We are again invoking the axiom of choice here.

where $\|\cdot\|$ denote the operator norm and \mathbf{Y}^\dagger is the Moore–Penrose pseudo-inverse of \mathbf{Y} . Equivalently, these are the largest and smallest singular values of $(2/\sqrt{m})\mathbf{Y}$.

The following is a slight edit of [11, Cor 2].

Lemma 5.3. *Consider $y_1, \dots, y_m \in \mathbb{R}^k$ with diameter ζ and width ω as defined in (5.3), and with pairwise distances denoted $\delta_{ij} := \|y_i - y_j\|$. For an arbitrary set of nonnegative numbers (λ_{ij}) , let $\eta^2 = \max_{i,j} |\lambda_{ij}^2 - \delta_{ij}^2|$. There is a constant $C > 0$ depending only on k such that, if $\eta/\omega \leq 1/C$, then Classical Scaling with input dissimilarities $\{\lambda_{ij}\}$ (and dimension k) returns a point set $z_1, \dots, z_m \in \mathbb{R}^k$ satisfying*

$$\min_{Q \in \mathbb{Q}_k} \left[\frac{1}{m} \sum_{i \in [m]} \|z_i - Q(y_i)\|^2 \right]^{1/2} \leq C(\zeta/\omega^2) \eta^2. \quad (5.4)$$

The following is a slightly different variant of [11, Cor 3].

Lemma 5.4. *Consider $y_1, \dots, y_m \in \mathbb{R}^k$ with diameter ζ and width ω as defined in (5.3). For a point $y \in \mathbb{R}^k$, set $\delta_i = \|y - y_i\|$. For another point set $z_1, \dots, z_m \in \mathbb{R}^k$ and an arbitrary set of nonnegative numbers (λ_i) , let $\xi^2 = \frac{1}{m} \sum_{i \in [m]} \|z_i - y_i\|^2$ and $\eta^2 = \max_i |\lambda_i^2 - \delta_i^2|$. There is a constant $C > 0$ depending only on k such that, if $\xi/\omega \leq 1/C$, Gower’s lateration with inputs (z_1, \dots, z_m) and (λ_i) returns $z \in \mathbb{R}^k$ satisfying*

$$\|z - y\| \leq (C/\omega)(\eta^2 + m\zeta\xi).$$

The reason we do not deal directly with Classical Scaling is because, in our setting, the width as defined in (5.3) cannot be controlled for the entire sample \mathbf{X} , so that the bound (5.4) is not directly useful to control the performance of Classical Scaling. Instead, we employ landmark Classical Scaling and prove the following more general result.

Theorem 5.5. *Starting from an estimate of the distances (\hat{d}_{ij}) satisfying (1.4), for each set of $k+1$ sample points, embed them by Classical Scaling and compute their width as in (5.3). Apply landmark Classical Scaling to (\hat{d}_{ij}) with the $(k+1)$ -tuple that gives the largest width as landmarks. There is a constant $C > 0$ depending on \mathcal{M} such that, if $\varepsilon \leq 1/C$, the resulting embedding satisfies the error bound (5.1).*

Proof. We start with the landmark points. First, we lower bound their width by a constant that only depends on \mathcal{M} . Let $\mathbf{A} = \{a_1, \dots, a_{k+1}\} \subset \mathcal{U}$ be such that its convex hull has maximum width among all $(k+1)$ -tuples in \mathcal{U} . Because \mathbf{U} is an ε -covering of \mathcal{U} , there are $u_{i_1}, \dots, u_{i_{k+1}}$ such that $\|a_j - u_{i_j}\| \leq \varepsilon$ for all $j \in [k+1]$. Assume without loss of generality that $i_j = j$ for all $j \in [k+1]$. Define $\mathbf{L} = \{u_1, \dots, u_{k+1}\}$. Given that $\text{width}_2(\mathbf{A})$ and $\text{width}_2(\mathbf{L})$ are the smallest singular values of $(1/\sqrt{k+1})\mathbf{A}$ and $(1/\sqrt{k+1})\mathbf{L}$, respectively, Weyl’s inequality gives

$$\text{width}_2(\mathbf{L}) \geq \text{width}_2(\mathbf{A}) - \frac{1}{\sqrt{k+1}} \|\mathbf{A} - \mathbf{L}\|.$$

We then have

$$\|\mathbf{A} - \mathbf{L}\|^2 \leq \|\mathbf{A} - \mathbf{L}\|_F^2 = \sum_{j \in [k+1]} \|a_j - u_j\|^2 \leq (k+1)\varepsilon^2,$$

so that

$$\omega := \text{width}_2(\mathbf{L}) \geq \text{width}_2(\mathbf{A}) - \varepsilon.$$

By construction, $\text{width}_2(\mathbf{A})$ is a constant of \mathcal{M} , say $2/C_1$, and henceforth we require that $\varepsilon \leq 1/C_1$ so that the landmarks have width $\omega \geq 1/C_1$ when embedded without error.

We now embed the landmark (or base) points \mathbf{L} by Classical Scaling. Let $\hat{u}_1, \dots, \hat{u}_{k+1}$ denote the embedded points. The embedding cannot be perfect as we do not know the true distances,

but only have access to estimates. (We are about to apply Lemma 5.3 with $y_i \leftarrow u_i$ so that $\delta_{ij} = \|u_i - u_j\| = d_{\mathcal{M}}(x_i, x_j)$, and $\lambda_{ij} \leftarrow \hat{d}_{ij}$, and the resulting embedding is $z_i \leftarrow \hat{u}_i$. We denote by C_3 the constant in that lemma.) Define

$$\eta^2 := \max_{i,j \in [k+1]} |\hat{d}_{ij}^2 - \|u_i - u_j\|^2| \leq C_2 \varepsilon^2, \quad (5.5)$$

by (1.4) and the fact that \mathcal{U} has a diameter that is a constant of \mathcal{M} , we apply Lemma 5.3 to get that, if $\eta/\omega \leq 1/C_3$, which holds if $\varepsilon \leq 1/(C_1 C_2^{1/2} C_3)$, then

$$\min_{Q \in \mathbb{Q}_k} \left[\frac{1}{k+1} \sum_{i \in [k+1]} \|\hat{u}_i - Q(u_i)\|^2 \right]^{1/2} \leq C_3 (\text{diam}_2(\mathbf{L})/\omega^2) \eta^2 \leq C_4 \varepsilon^2,$$

again using the fact that $\omega \geq 1/C_1$ and $\text{diam}_2(\mathbf{L}) \leq \text{diam}(\mathcal{U})$, which is a constant of \mathcal{M} . Henceforth, we assume that $Q = \text{id}$ without loss of generality so that

$$\xi^2 := \frac{1}{k+1} \sum_{i \in [k+1]} \|\hat{u}_i - u_i\|^2 \leq (C_4 \varepsilon^2)^2. \quad (5.6)$$

Finally, we embed the remaining points, $x_i, i > k+1$, one-by-one by lateration. This is done by reference to $\hat{u}_1, \dots, \hat{u}_{k+1}$ using the estimated distances (\hat{d}_{ij}) . Take p in $\{k+2, \dots, n\}$ and consider embedding x_p . (We are about to apply Lemma 5.4 with $y_i \leftarrow u_i$ for $i \in [k+1]$ and $y = u_p$ for some $p > k+1$, so that $\delta_i = \|u_p - u_i\| = d_{\mathcal{M}}(x_p, x_i)$, and $z_i \leftarrow \hat{u}_i$ and $\lambda_i = \hat{d}_{pi}$. We denote by C_5 the constant in that lemma.) If $\xi/\omega \leq 1/C_5$, which in view of (5.6) holds if $\varepsilon \leq 1/(C_1^{1/4} C_4^{1/2} C_5^{1/2})$, then

$$\|\hat{u}_p - u_p\| \leq (C_5/\omega)(\eta^2 + (k+1)\zeta\xi) \leq C_1 C_5 (C_2 \varepsilon^2 + (k+1) \text{diam}(\mathcal{U}) C_4 \varepsilon^2) =: C_6 \varepsilon^2.$$

using $\omega \geq 1/C_1$, (5.5), (5.6), and $\text{diam}_2(\mathbf{L}) \leq \text{diam}(\mathcal{U})$, which is a constant of \mathcal{M} . \square

Remark 5.6. The procedure described in Theorem 5.5 would in principle require going all possible $(k+1)$ -tuples, and there are too many of them (on the order of $O(n^{k+1})$) for this to be practical. In principle, a randomized version would do essentially as well. It would amount to examining a number N of $(k+1)$ -tuples and choosing the best among them in terms of width. Then, the error bound (5.1) would hold, say with twice the constant there, with probability exponentially close to 1 as a function of N . Another possibility is to subsample \mathbf{X} to obtain an $(2\varepsilon, 1/2)$ -net (see Section 4.1) and embed it by Classical Scaling — which turns out to be fine in that case. Once embedded, it is computationally much easier to select a $(k+1)$ -tuple of points with good width, and these are used to embedding the remaining sample points by lateration.

5.2 Information bound

The same example used in Section 3.2 can also be used to establish an information bound showing that the stated performance bound established in Theorem 5.2 is best possible. Indeed, using some of the same notation, on the one hand, \mathcal{M}_1 is isometric to $\mathcal{U}_1 := [0, 1]^k$, with corresponding embedded points $u_i^1 := (x_{i,1}, \dots, x_{i,k})$ when $x_i = (x_{i,1}, \dots, x_{i,k})$. On the other hand, \mathcal{M}_2 is isometric to $\mathcal{U}_2 := [0, 1]^{k-1} \times [0, \Lambda(\gamma_\varepsilon)]$, with corresponding embedded points $u_i^2 := (x_{i,1}, \dots, x_{i,k-1}, \lambda_\varepsilon(x_{i,k}))$, where λ_ε is defined in (3.3). These embeddings are obviously not the only possibilities, but any other ones would have to be obtained by rigid transformations of these, and these particular ones are closest in average squared distance. See Lemma 5.8 below.

We then proceed to lower bound the squared average distance between these two embeddings

$$\begin{aligned}
\max_{i \in [m]^k} \|u_i^1 - u_i^2\|^2 &\geq \frac{1}{m^k} \sum_{i \in [m]^k} \|u_i^1 - u_i^2\|^2 = \frac{1}{m^k} \sum_{i \in [m]^k} [x_{i,k} - \lambda_\varepsilon(x_{i,k})]^2 \\
&= \frac{1}{m} \sum_{j \in [m]} [(j-1)\varepsilon - (j-1)\eta]^2 \\
&= \frac{1}{m} (\varepsilon - \eta)^2 \sum_{j \in [m]} (j-1)^2 \\
&= (\varepsilon - \eta)^2 (2m-1)(m-1) \geq C_1^2 \varepsilon^4,
\end{aligned}$$

using at the end the lower bound in (3.2) and the fact that $\varepsilon = 1/(m-1)$.

Based on what we know of the true \mathcal{M} , it could be \mathcal{M}_1 as easily as \mathcal{M}_2 , and therefore, for any embedding \hat{u}_i ,

$$\begin{aligned}
\max_{\mathcal{M} \in \{\mathcal{M}_1, \mathcal{M}_2\}} \min_{Q \in \mathbb{Q}_k} \max_{i \in [n]} \|\hat{u}_i - Q(u_i)\| &= \max \left\{ \min_{Q \in \mathbb{Q}_k} \max_{i \in [n]} \|\hat{u}_i - Q(u_i^1)\|, \min_{Q \in \mathbb{Q}_k} \max_{i \in [n]} \|\hat{u}_i - Q(u_i^2)\| \right\} \\
&\geq \frac{1}{2} \min_{Q \in \mathbb{Q}_k} \max_{i \in [n]} \|u_i^1 - Q(u_i^2)\| \\
&= \frac{1}{2} \max_{i \in [n]} \|u_i^1 - u_i^2\| \\
&\geq \frac{1}{2} C_1 \varepsilon^2.
\end{aligned}$$

We have thus established the following.

Theorem 5.7. *For any embedding method \hat{u} , the following is true. For any $\varepsilon > 0$, there is a surface \mathcal{M} satisfying Assumption 5.1 and a set of points x_1, \dots, x_n belonging to \mathcal{M} dense enough that (1.1) holds, such that*

$$\min_{Q \in \mathbb{Q}_k} \max_{i \in [n]} \|\hat{u}_i - Q(u_i)\| \geq C^{-1} \varepsilon^2.$$

Lemma 5.8. *Consider two sets of points, $u_i = i = (i_1, \dots, i_k)$ and $v_i := (\alpha_1 i_1, \dots, \alpha_k i_k)$ for $i \in [m]^k$ and some real numbers $\alpha_1, \dots, \alpha_k$. Then, regardless of α , the best alignment of these points by a rigid transformation is achieved by the identity transformation.*

Proof. The optimization problem we are studying is

$$\min_{Q \in \mathbb{Q}_k} \sum_{i \in [m]^k} \|v_i - Q(u_i)\|^2 = \min_{R \in \mathbb{O}_k} \min_{r \in \mathbb{R}^k} \sum_{i \in [m]^k} \|v_i - r - Ru_i\|^2,$$

where \mathbb{O}_k is the class of orthogonal transformations of \mathbb{R}^k . Given R , the minimum over r is achieved at the average of $v_i - Ru_i$, which reduces the problem to

$$\min_{R \in \mathbb{O}_k} \sum_{i \in [m]^k} \|v_i - \bar{v} - R(u_i - \bar{u})\|^2,$$

where $\bar{u} := (\frac{m+1}{2}, \dots, \frac{m+1}{2})$ and $\bar{v} := (\alpha_1 \frac{m+1}{2}, \dots, \alpha_k \frac{m+1}{2})$ are the barycenters of u_1, \dots, u_n and v_1, \dots, v_n , respectively. Let U and V be the matrices with row vectors $u_i - \bar{u}$ and $v_i - \bar{v}$, respectively. It is well-known that the optimal orthogonal transformation solving the problem the optimal R above is AB^\top if ΛAB^\top is a singular value decomposition of $M := V^\top U$. To show that this is the identity matrix, it suffices to show that M is diagonal, or equivalently, that the canonical basis

Algorithm 1 Mesh Isomap

Input: point set x_1, \dots, x_n in \mathbb{R}^d , embedding dimension k , any parameter of `mesh`

Output: point set $\hat{u}_1, \dots, \hat{u}_n$ in \mathbb{R}^k

1: Apply `mesh` to x_1, \dots, x_n to get a mesh \hat{M}

2: Apply `meshDistances` to \hat{M} to get a matrix of pairwise distances \hat{D}

3: Apply MDS to \hat{D} to produce a point set u_1, \dots, u_n in \mathbb{R}^k

Return: the point set $\hat{u}_1, \dots, \hat{u}_n$

vectors of \mathbb{R}^k , denoted e_1, \dots, e_k below, are eigenvectors for M . Take any $t \in [k]$. Then, noting that $M = \sum_i (v_i - \bar{v})(u_i - \bar{u})^\top$, we have for $s \neq t$,

$$\begin{aligned} (Me_t)_s &= \sum_{i \in [m]^k} (v_i - \bar{v})_s (u_i - \bar{u})_t \\ &= \sum_{i \in [m]^k} \alpha_s (i_s - \frac{m+1}{2}) (i_t - \frac{m+1}{2}) \\ &= m^{k-2} \alpha_s \sum_{i_s \in [m]} (i_s - \frac{m+1}{2}) \sum_{i_t \in [m]} (i_t - \frac{m+1}{2}) = 0, \end{aligned}$$

and, similarly,

$$(Me_t)_t = m^{k-1} \alpha_t \sum_{i_t \in [m]} (i_t - \frac{m+1}{2})^2 =: a \alpha_t, \quad a := m^k(m^2 - 1)/12.$$

Hence, $Me_t = a \alpha_t e_t$, so that e_t is indeed an eigenvector of M (for the eigenvalue $a \alpha_t$). \square

5.3 Mesh Isomap

Isomap consists in 1) building a neighborhood graph; 2) computing all pairwise graph distances; 3) applying Classical Scaling to the resulting distances. Steps 1 and 2 have for purpose to estimate the pairwise intrinsic distances on the underlying surface, and this is where we bring an improvement, as we replace these steps with a more accurate way of estimating distances based on a mesh construction. Step 3 remains the same in principle, or it can be replaced by any other method for MDS as was done for Isomap, where landmark Classical Scaling was proposed as a faster alternative [73]. See Algorithm 1, where `mesh` denotes a generic mesh construction algorithm and `meshDistances` a generic algorithm for computing all pairwise distances between the vertices of a given mesh, and MDS denotes a generic method for MDS.

Remark 5.9. Although the method as such seems new, it was mentioned in [15] in a discussion of the original Isomap paper [78]. In that discussion, the authors mention previous work of theirs [70] on the flattening of a mesh, which consists in computing the distances on the mesh and then applying the multidimensional scaling method of [69]. Note however that the setting is different in that a mesh is assumed to be provided, while we only assume that a point cloud is provided. Although this distinction was immediately underscored by the authors of Isomap in their rebuttal, they also failed to realize that a better performance could be gained by using a mesh construction in the process of computing the pairwise distances. This is the main novelty in Algorithm 1.

In an effort to obtain a performance bound for Mesh Isomap, we specialize the algorithm by using as mesh construction the tangential Delaunay complex corrected for inconsistencies based on estimated tangent spaces described in Section 4.2 and using as method for MDS landmark Classical Scaling as described in Section 5.1.

We established in Theorem 4.7 that the mesh construction yields distance estimates that satisfy (1.4), but we did so under the assumption that the surface \mathcal{M} does not have a boundary. It turns out that the construction is local in that the computation of a given simplex in the complex only depends on the sample points that are within $C_1\varepsilon$ of the simplex [21, Lem 8.10(3)]; and the estimation of the tangent spaces at a given point, as carried out in Section 4.3.1, only depends on the sample points that are within $C_2\varepsilon$ of the point of interest. This leads us to anticipate that the embedding error (5.1) applies here as well — even though \mathcal{M} has a boundary — at least for data points that are $C_3\varepsilon$ away from $\partial\mathcal{M}$. This points to the possibility that *this variant of Mesh Isomap is minimax rate-optimal for manifold learning in the situation where the submanifold is isometric to a convex domain*.

5.4 Numerical experiments

In this subsection, we compare the original Isomap algorithm with Mesh Isomap in simulations. We do so on the Swiss roll, which is perhaps the most emblematic surface in manifold learning. In our implementation of Mesh Isomap we used the same tangential Delaunay complex construction [50] as we did in Section 4.4. The embedding error was computed up to a rigid transformation by Procrustes.

The result of this experiment is reported in Figure 5.1. As in Section 4.4, the average performance of Mesh Isomap is noticeably better than that of regular Isomap across all choices of the connectivity radius.

6 Discussion

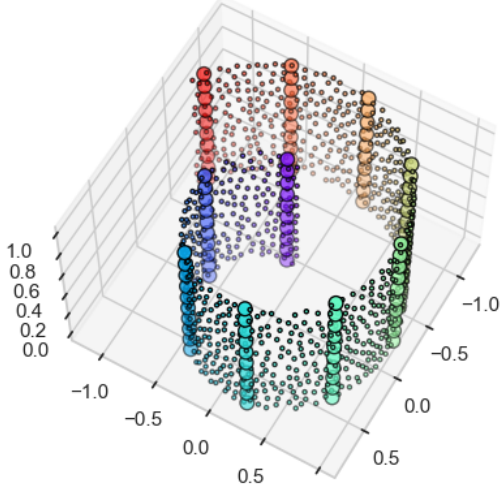
In two places in the paper, we suspected but were not able to prove that surfaces were $O(\varepsilon^2)$ -distortions of each other — and had to use a different route to get to the desired result.

In Section 3, we believe that $\hat{\mathcal{M}}$ and \mathcal{M} are $O(\varepsilon^2)$ -distortions of each other. If this had been established, then it would have enabled us to apply Corollary 2.3 to immediately get Theorem 3.3. As we were not able to prove this claim, we used a different route through Lemma 2.5 instead.

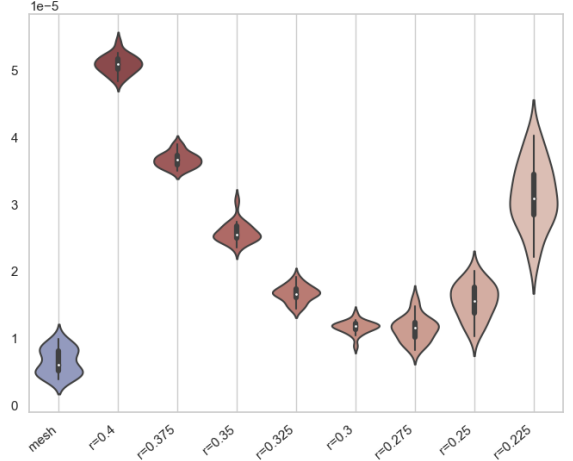
Conjecture 6.1. There are universal constants $C_1, C_2 > 0$ such that, if \mathcal{M} and \mathcal{S} are compact and connected k -dimensional submanifolds without boundary with $\text{reach} \geq \rho$, and if they are within Hausdorff distance $h \leq \rho/C_1$ of each other, then they are $(C_2 h/\rho)$ -distortions of each other.

In Section 4, we believe that $\hat{\mathcal{T}}_c$ and \mathcal{M} are $O(\varepsilon^2)$ -distortions of each other. (In [2, Th 4.1] and its proof via [2, Lem 4.2], we see that \mathcal{M} and $\tilde{\mathcal{M}}$ are $O(\varepsilon)$ -distortions of each other. It would have been enough to have $O(\varepsilon^2)$ in place of $O(\varepsilon)$.) If this had been established, then it would have enabled us to apply Corollary 2.3 to immediately get Theorem 4.7. Although the proof of that result is short, we could have avoided the use of multiple net construction as described in Section 4.1 — see Remark 4.2 there. It would have been enough to work with a single net (obtained by subsampling \mathbf{X}) and then the error bound (1.4) would have been established for all sample points (including those outside the net) by way of Corollary 2.3.

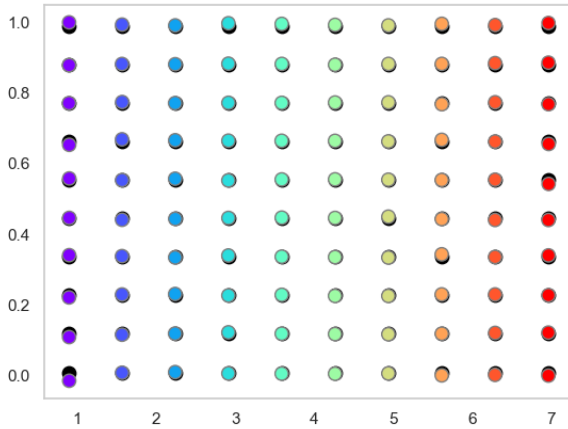
Conjecture 6.2. There are universal constants $C_1, C_2 > 0$ such that the following holds. Suppose \mathcal{M} is a compact and connected k -dimensional submanifold without boundary with $\text{reach} \geq \rho$. Consider a k -simplicial complex \mathcal{T} with vertices on \mathcal{M} that is homeomorphic to \mathcal{M} and such that all its k -simplexes have diameter $\leq h$ with $h/\rho \leq 1/C_1$ and thickness $\geq 1/C_1$. Then they are $(C_2 h/\rho)$ -distortions of each other.



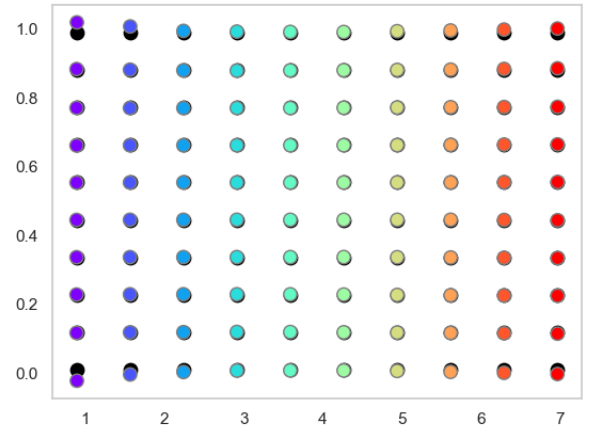
(a) The large colored points on the Swiss roll (of sample size $n = 1000$) are the landmarks that will be embedded in \mathbb{R}^2 using Classical Scaling.



(b) Procrustes error of the embeddings returned by Mesh Isomap (blue) and regular Isomap with varying connectivity radius. The graph approximation provides the most accurate embedding with $r = 0.3$, but the mesh approximation is more accurate still. Based on 20 repeats.



(c) Typical output of regular Isomap with the best choice of neighborhood radius $r = 0.3$. The original points are in black and the output is in color.



(d) Typical output of Mesh Isomap. The original points are in black and the output is in color.

Figure 5.1: Comparison of Isomap and Mesh Isomap on the Swiss roll.

Acknowledgments

When EAC presented prior work on this topic at the *6th Princeton Day of Statistics*, Amit Moscovich proposed this idea of using an approximation to the underlying surface to possibly obtain a better approximation rate, which is at the foundation of the present paper. Although we later discovered that this idea had been entertained earlier (see Remark 5.9), we are nonetheless indebted to him as this idea got us started on this project. We are also grateful to Eddie Aamari, Jean-Daniel Boissonnat, Frédéric Chazal, and Justin Roberts for helpful discussions and pointers to the literature. This work was partially supported by the US National Science Foundation (DMS 1916071).

References

- [1] E. Aamari, C. Berenfeld, and C. Levrard. Optimal reach estimation and metric learning. *arXiv preprint arXiv:2207.06074*, 2022.
- [2] E. Aamari and C. Levrard. Stability and minimax optimality of tangential Delaunay complexes for manifold reconstruction. *Discrete & Computational Geometry*, 59(4):923–971, 2018.
- [3] C. Aaron and O. Bodart. Convergence rates for estimators of geodesic distances and fréchet expectations. *Journal of Applied Probability*, 55(4):1001–1013, 2018.
- [4] N. M. Amato and G. Song. Using motion planning to study protein folding pathways. *Journal of Computational Biology*, 9(2):149–168, 2002.
- [5] N. Amenta. The crust algorithm for 3-D surface reconstruction. In *Symposium on Computational Geometry*, pages 423–424, 1999.
- [6] N. Amenta and M. Bern. Surface reconstruction by voronoi filtering. *Discrete & Computational Geometry*, 22(4):481–504, 1999.
- [7] N. Amenta, M. Bern, and D. Eppstein. The crust and the beta-skeleton: Combinatorial curve reconstruction. In *Graphical Models and Image Processing*, pages 125–135, 1998.
- [8] N. Amenta, M. Bern, and M. Kamvysselis. A new Voronoi-based surface reconstruction algorithm. In *Proceedings of the 25th Annual Conference on Computer Graphics and Interactive Techniques*, pages 415–421, 1998.
- [9] N. Amenta, S. Choi, T. K. Dey, and N. Leekha. A simple algorithm for homeomorphic surface reconstruction. In *Proceedings of the Sixteenth Annual Symposium on Computational Geometry*, pages 213–222, 2000.
- [10] N. Amenta, S. Choi, and R. K. Kolluri. The power crust. In *Proceedings of the Sixth ACM Symposium on Solid Modeling and Applications*, pages 249–266, 2001.
- [11] E. Arias-Castro, A. Javanmard, and B. Pelletier. Perturbation bounds for procrustes, classical scaling, and trilateration, with applications to manifold learning. *Journal of Machine Learning Research*, 21:1–37, 2020.
- [12] E. Arias-Castro and T. Le Gouic. Unconstrained and curvature-constrained shortest-path distances and their approximation. *Discrete & Computational Geometry*, 62(1):1–28, 2019.
- [13] E. Arias-Castro, G. Lerman, and T. Zhang. Spectral clustering based on local PCA. *The Journal of Machine Learning Research*, 18(1):253–309, 2017.
- [14] E. Arias-Castro and B. Pelletier. On the convergence of maximum variance unfolding. *The Journal of Machine Learning Research*, 14(1):1747–1770, 2013.
- [15] M. Balasubramanian and E. Schwartz. The isomap algorithm and topological stability. *Science*, 295(5552):7a, 2002.
- [16] M. Belkin and P. Niyogi. Laplacian eigenmaps for dimensionality reduction and data representation. *Neural Computation*, 15(16):1373–1396, 2003.
- [17] M. Belkin and P. Niyogi. Towards a theoretical foundation for Laplacian-based manifold methods. *Journal of Computer and System Sciences*, 74(8):1289–1308, 2008.
- [18] F. Bernardini, J. Mittleman, H. Rushmeier, C. Silva, and G. Taubin. The ball-pivoting algorithm

- for surface reconstruction. *IEEE Transactions on Visualization and Computer Graphics*, 5(4):349–359, 1999.
- [19] M. Bernstein, V. De Silva, J. Langford, and J. Tenenbaum. Graph approximations to geodesics on embedded manifolds. Technical report, Department of Psychology, Stanford University, 2000.
 - [20] J.-D. Boissonnat and F. Cazals. Smooth surface reconstruction via natural neighbour interpolation of distance functions. *Computational Geometry*, 22(1-3):185–203, 2002.
 - [21] J.-D. Boissonnat, F. Chazal, and M. Yvinec. *Geometric and Topological Inference*. Cambridge University Press, 2018.
 - [22] J.-D. Boissonnat, R. Dyer, and A. Ghosh. Delaunay triangulation of manifolds. *Foundations of Computational Mathematics*, 18(2):399–431, 2018.
 - [23] J.-D. Boissonnat and J. Flototto. A local coordinate system on a surface. In *Proceedings of the Seventh ACM Symposium on Solid Modeling and Applications*, SMA '02, pages 116–126, New York, NY, USA, 2002. Association for Computing Machinery.
 - [24] J.-D. Boissonnat and J. Flötotto. A coordinate system associated with points scattered on a surface. *Computer-Aided Design*, 36(2):161–174, 2004.
 - [25] J.-D. Boissonnat and A. Ghosh. Manifold reconstruction using tangential Delaunay complexes. *Discrete & Computational Geometry*, 51(1):221–267, 2014.
 - [26] V. Borrelli, S. Jabrane, F. Lazarus, and B. Thibert. Isometric embeddings of the square flat torus in ambient space. *Ensaïos Matemáticos*, 24:1–91, 2013.
 - [27] M. Brand. Charting a manifold. *Advances in Neural Information Processing Systems*, pages 985–992, 2003.
 - [28] J. Chen and Y. Han. Shortest paths on a polyhedron. In *Proceedings of the Sixth Annual Symposium on Computational Geometry*, pages 360–369, 1990.
 - [29] S.-W. Cheng, T. K. Dey, H. Edelsbrunner, M. A. Facello, and S.-H. Teng. Sliver exudation. *Journal of the ACM*, 47(5):883–904, 2000.
 - [30] R. Coifman and S. Lafon. Diffusion maps. *Applied and Computational Harmonic Analysis*, 21(1):5–30, 2006.
 - [31] G. Csardi and T. Nepusz. The igraph software package for complex network research. *Interjournal, Complex Systems*:1695, 2006.
 - [32] V. de Silva and J. B. Tenenbaum. Sparse multidimensional scaling using landmark points. Technical report, Technical report, Stanford University, 2004.
 - [33] T. K. Dey and S. Goswami. Tight cocone: a water-tight surface reconstructor. *Journal of Computing and Information Science in Engineering*, 3(4):302–307, 2003.
 - [34] T. K. Dey and S. Goswami. Provable surface reconstruction from noisy samples. *Computational Geometry*, 35(1-2):124–141, 2006.
 - [35] T. K. Dey, K. Li, E. A. Ramos, and R. Wenger. Isotopic reconstruction of surfaces with boundaries. In *Computer Graphics Forum*, volume 28, pages 1371–1382. Wiley Online Library, 2009.
 - [36] J. Digne. An analysis and implementation of a parallel ball pivoting algorithm. *Image Processing on Line*, 4:149–168, 2014.
 - [37] V. Divol. Minimax adaptive estimation in manifold inference. *Arxiv Preprint Arxiv:2001.04896*, 2020.
 - [38] D. Donoho and C. Grimes. Hessian eigenmaps: Locally linear embedding techniques for high-dimensional data. *Proceedings of the National Academy of Sciences*, 100(10):5591–5596, 2003.
 - [39] L. E. Dubins. On curves of minimal length with a constraint on average curvature, and with prescribed initial and terminal positions and tangents. *American Journal of Mathematics*, 79(3):497–516, 1957.
 - [40] R. Dyer, G. Vegter, and M. Wintraecken. Riemannian simplices and triangulations. *Geometriae Dedicata*, 179(1):91–138, 2015.
 - [41] H. Federer. Curvature measures. *Transactions of the American Mathematical Society*, 93(3):418–491, 1959.
 - [42] D. Freedman. Efficient simplicial reconstructions of manifolds from their samples. *IEEE Transactions on Pattern Analysis and Machine Intelligence*, 24(10):1349–1357, 2002.
 - [43] K. Fukunaga and D. R. Olsen. An algorithm for finding intrinsic dimensionality of data. *IEEE Transactions on Computers*, 100(2):176–183, 1971.
 - [44] C. R. Genovese, M. Perone-Pacifico, I. Verdinelli, L. Wasserman, et al. Manifold estimation and singular deconvolution under Hausdorff loss. *The Annals of Statistics*, 40(2):941–963, 2012.

- [45] E. Giné and V. Koltchinskii. Empirical graph Laplacian approximation of Laplace–Beltrami operators: Large sample results. In *High Dimensional Probability*, pages 238–259. Institute of Mathematical Statistics, 2006.
- [46] Y. Goldberg, A. Zakai, D. Kushnir, and Y. Ritov. Manifold learning: The price of normalization. *Journal of Machine Learning Research*, 9(Aug):1909–1939, 2008.
- [47] J. C. Gower. Adding a point to vector diagrams in multivariate analysis. *Biometrika*, 55(3):582–585, 1968.
- [48] M. Hein, J.-Y. Audibert, and U. von Luxburg. From graphs to manifolds – weak and strong pointwise consistency of graph laplacians. In P. Auer and R. Meir, editors, *Learning Theory*, volume 3559 of *Lecture Notes in Computer Science*, pages 470–485. Springer Berlin / Heidelberg, 2005.
- [49] H. Hoppe, T. DeRose, T. Duchamp, J. McDonald, and W. Stuetzle. Surface reconstruction from unorganized points. *ACM SIGGRAPH Computer Graphics*, 26(2):71–78, July 1992.
- [50] C. Jamin. Tangential complex. In *GUDHI User and Reference Manual*. GUDHI Editorial Board, 3.2.0 edition, 2020.
- [51] L. Janson, B. Ichter, and M. Pavone. Deterministic sampling-based motion planning: Optimality, complexity, and performance. *The International Journal of Robotics Research*, 37(1):46–61, 2018.
- [52] N. Kambhatla and T. K. Leen. Dimension reduction by local principal component analysis. *Neural Computation*, 9(7):1493–1516, 1997.
- [53] L. Kaufman and P. Rousseeuw. Clustering by means of medoids. In *Statistical Data Analysis Based on the L_1 Norm Conference, Neuchatel, 1987*, pages 405–416, 1987.
- [54] S. Kiazky, S. Lorient, and É. C. de Verdière. Triangulated surface mesh shortest paths. In *CGAL User and Reference Manual*. CGAL Editorial Board, 5.1 edition, 2020.
- [55] A. K. Kim, H. H. Zhou, et al. Tight minimax rates for manifold estimation under Hausdorff loss. *Electronic Journal of Statistics*, 9(1):1562–1582, 2015.
- [56] J. Kim, A. Rinaldo, and L. Wasserman. Minimax rates for estimating the dimension of a manifold. *Journal of Computational Geometry*, 10(1), 2019.
- [57] J. B. Kruskal and J. B. Seery. Designing network diagrams. In *Conference on Social Graphics*, pages 22–50, 1980.
- [58] J.-C. Latombe. *Robot Motion Planning*, volume 124. Springer, 2012.
- [59] S. M. LaValle. *Planning Algorithms*. Cambridge University Press, 2006.
- [60] D. Li and D. B. Dunson. Geodesic distance estimation with spherelets. *Arxiv Preprint Arxiv:1907.00296*, 2019.
- [61] L. v. d. Maaten and G. Hinton. Visualizing data using t-SNE. *Journal of Machine Learning Research*, 9(Nov):2579–2605, 2008.
- [62] L. McInnes, J. Healy, N. Saul, and L. Großberger. Umap: Uniform manifold approximation and projection. *Journal of Open Source Software*, 3(29):861, 2018.
- [63] B. Mederos, N. Amenta, L. Velho, and L. H. De Figueiredo. Surface reconstruction for noisy point clouds. In *Symposium on Geometry Processing*, pages 53–62, 2005.
- [64] D. Niculescu and B. Nath. DV based positioning in ad hoc networks. *Telecommunication Systems*, 22(1-4):267–280, 2003.
- [65] S. Oh, A. Montanari, and A. Karbasi. Sensor network localization from local connectivity: Performance analysis for the MDS-map algorithm. In *Information Theory, 2010 IEEE Information Theory Workshop On*, pages 1–5. IEEE, 2010.
- [66] A. Paprotny and J. Garcke. On a connection between maximum variance unfolding, shortest path problems and isomap. In *Artificial Intelligence and Statistics*, pages 859–867, 2012.
- [67] H.-S. Park and C.-H. Jun. A simple and fast algorithm for k-medoids clustering. *Expert Systems with Applications*, 36(2):3336–3341, 2009.
- [68] S. Roweis and L. Saul. Nonlinear dimensionality reduction by locally linear embedding. *Science*, 290(5500):2323–2326, 2000.
- [69] J. W. Sammon. A nonlinear mapping for data structure analysis. *IEEE Transactions on Computers*, 100(5):401–409, 1969.
- [70] E. Schwartz, A. Shaw, and E. Wolfson. A numerical solution to the generalized mapmaker’s problem: flattening nonconvex polyhedral surfaces. *Pattern Analysis and Machine Intelligence, IEEE Transactions On*, 11(9):1005–1008, 1989.

- [71] Y. Shang and W. Ruml. Improved MDS-based localization. In *Conference of the IEEE Computer and Communications Societies*, volume 4, pages 2640–2651. IEEE, 2004.
- [72] Y. Shang, W. Ruml, Y. Zhang, and M. P. Fromherz. Localization from mere connectivity. In *ACM International Symposium on Mobile Ad Hoc Networking and Computing*, pages 201–212, 2003.
- [73] V. Silva and J. Tenenbaum. Global versus local methods in nonlinear dimensionality reduction. *Advances in Neural Information Processing Systems*, 15:705–712, 2002.
- [74] A. Singer. From graph to manifold Laplacian: The convergence rate. *Applied and Computational Harmonic Analysis*, 21(1):128–134, 2006.
- [75] A. Smith, X. Huo, and H. Zha. Convergence and rate of convergence of a manifold-based dimension reduction algorithm. In *Advances in Neural Information Processing Systems*, pages 1529–1536, 2008.
- [76] G. W. Stewart and J. G. Sun. *Matrix Perturbation Theory*. Computer Science and Scientific Computing. Academic Press Inc., Boston, MA, 1990.
- [77] J. Tenenbaum. Mapping a manifold of perceptual observations. *Advances in neural information processing systems*, 10, 1997.
- [78] J. B. Tenenbaum, V. De Silva, and J. C. Langford. A global geometric framework for nonlinear dimensionality reduction. *Science*, 290(5500):2319–2323, 2000.
- [79] S. Thomas, G. Song, and N. M. Amato. Protein folding by motion planning. *Physical Biology*, 2(4):S148, 2005.
- [80] W. S. Torgerson. *Theory and Methods of Scaling*. Wiley, 1958.
- [81] U. von Luxburg, M. Belkin, and O. Bousquet. Consistency of spectral clustering. *The Annals of Statistics*, 36(2):555–586, 2008.
- [82] K. Weinberger, F. Sha, and L. Saul. Learning a kernel matrix for nonlinear dimensionality reduction. In *International Conference on Machine Learning*, page 106, 2004.
- [83] A. Weingessel and K. Hornik. Local pca algorithms. *IEEE Transactions on Neural Networks*, 11(6):1242–1250, 2000.
- [84] H. Whitney. *Geometric Integration Theory*. Princeton University Press, 1957.
- [85] S.-Q. Xin and G.-J. Wang. Improving Chen and Han’s algorithm on the discrete geodesic problem. *ACM Transactions on Graphics*, 28(4):1–8, 2009.
- [86] Q. Ye and W. Zhi. Discrete Hessian eigenmaps method for dimensionality reduction. *Journal of Computational and Applied Mathematics*, 278:197–212, 2015.
- [87] H. Zha and Z. Zhang. Continuum isomap for manifold learnings. *Computational Statistics & Data Analysis*, 52(1):184–200, 2007.
- [88] Z. Zhang and H. Zha. Principal manifolds and nonlinear dimension reduction via tangent space alignment. *SIAM Journal on Scientific Computing*, 26(1):313–338, 2004.